PRODUCTION AND CHARACTERIZATION OF MAGNESIUM OXYCHLORIDE CEMENT BASED POLISHING BRICKS FOR POLISHING OF CERAMIC TILES

A THESIS SUBMITTED TO
THE GRADUATE SCHOOL OF NATURAL AND APPLIED SCIENCES
OF
MIDDLE EAST TECHNICAL UNIVERSITY

BY

MUHAMMED SAİD ÖZER

IN PARTIAL FULFILLMENT OF THE REQUIREMENTS
FOR
THE DEGREE OF MASTER OF SCIENCE
IN
METALLURGICAL AND MATERIALS ENGINEERING

DECEMBER 2008

Approval of the thesis:

PRODUCTION AND CHARACTERIZATION OF MAGNESIUM OXYCHLORIDE CEMENT BASED POLISHING BRICKS FOR POLISHING OF CERAMIC TILES

submitted by **MUHAMMED SAİD ÖZER** in partial fulfillment of the requirements for the degree of **Master of Science in Metallurgical and Materials Engineering Department, Middle East Technical University** by,

Prof. Dr. Canan Özgen _____
Dean, Graduate School of **Natural and Applied Sciences**

Prof. Dr. Tayfur Öztürk _____
Head of Department, **Metallurgical and Materials Engineering**

Prof. Dr. Abdullah Öztürk _____
Supervisor, **Metallurgical and Materials Eng. Dept., METU**

Examining Committee Members:

Prof. Dr. Muharrem Timuçin _____
Metallurgical and Materials Engineering Dept., METU

Prof. Dr. Çetin Hoşten _____
Mining Engineering Dept., METU

Prof. Dr. Abdullah Öztürk _____
Metallurgical and Materials Engineering Dept., METU

Prof. Dr. Hakan Gür _____
Metallurgical and Materials Engineering Dept., METU

Assist. Prof. Dr. Caner Durucan
Metallurgical and Materials Engineering Dept., METU _____

Date: 15.12.2008

I hereby declare that all information in this document has been obtained and presented in accordance with academic rules and ethical conduct. I also declare that, as required by these rules and conduct, I have fully cited and referenced all material and results that are not original to this work.

Name, Last name : Muhammed Said Özer

Signature :

ABSTRACT

PRODUCTION AND CHARACTERIZATION OF MAGNESIUM OXYCHLORIDE CEMENT BASED POLISHING BRICKS FOR POLISHING OF CERAMIC TILES

Özer, Muhammed Said
M.S., Department of Metallurgical and Materials Engineering
Supervisor: Prof. Dr. Abdullah Öztürk

December 2008, 77 pages

Magnesium oxychloride cement (MOC) based grinding and polishing bricks developed for polishing of granite based ceramic tiles were produced and characterized. For surface grinding 46 and 180 grit size SiO_2 powder embedded MOC based abrasive bricks; for polishing 600 and 1200 grit size SiC powder embedded MOC based abrasive bricks followed by neat (unreinforced) MOC pastes were applied on ceramic tiles.

Three different neat MOC pastes depending on $MgO/MgCl_2$ molar ratio in the paste e.g. 6/1, 7/1, and 8/1, were formed and evaluated. Grinding bricks were formed by adding 30 weight percentage, wt%, of both SiO_2 powders. Polishing bricks were formed by adding 20, 25, and 30 wt% of both SiC powders. X-Ray diffraction analyses revealed that MOC F5 was the main crystalline phase in the neat MOC pastes.

Additions of both SiO_2 and SiC powders enhanced mechanical properties namely; compressive strength and abrasion resistance, chemical durability in water and polishing ability of MOC paste. More than 25 wt% addition of SiC powders had a tendency to decrease the compressive strength and water resistance of MOC paste. Polishing performance of abrasive bricks was evaluated in terms of mean surface roughness of ceramic tiles and abrasive brick consumption upon polishing. Scanning Electron Microscope examinations revealed the evidences of the reasons that 25 wt% SiC powder embedded abrasive bricks has the best qualifications in terms of abrasion resistance and polishing performance.

Keywords: Polishing, Granite, Ceramic Tile, Sorel Cement, Magnesium Oxychloride, Abrasive, Roughness.

ÖZ

SERAMİK KAROLARIN PARLATILMASINDA KULLANILACAK MAGNEZYUM OKSİKLORİT ESASLI PARLATMA PABUÇLARININ ÜRETİMİ VE KARAKTERİZASYONU

Özer, Muhammed Said
Yüksek Lisans, Metalurji ve Malzeme Mühendisliği Bölümü
Tez Yöneticisi: Prof. Dr. Abdullah Öztürk

Aralık 2008, 77 sayfa

Granit esaslı seramik karoların parlatılması için geliştirilmiş magnezyum oksiklorit çimento (MOC) esaslı aşındırma ve parlatma pabuçlarının üretildi ve karakterize edildi. Yüzey aşındırma işlemi için 46 ve 180 grit numaralı SiO_2 tozu katkılı MOC pabuçlar; parlatma işlemi için 600 ve 1200 grit numaralı SiC tozu katkılı MOC pabuçları takiben yalın (katkısız) MOC pastaları seramik karoların üzerine sıra ile uygulandı.

Çimento pastasının içerdiği $MgO/MgCl_2$ mol oranı 6/1, 7/1 ve 8/1 olacak şekilde üç ayrı MOC pastası hazırlandı ve değerlendirildi. Aşındırma pabuçları her bir SiO_2 tozundan ağırlıkça % 30 oranı ilave edilerek hazırlandı. Parlatma pabuçları ise her bir SiC tozundan çimentoya ağırlıkça % oranı 20, 25 ve 30 olacak şekilde ilave edilerek hazırlandı. X-Işınları kırınım analizleri yalın MOC pastalarında kristal yapının esas olarak F5 fazından oluştuğunu göstermiştir.

SiO_2 ve SiC tozlarının ilavesi MOC pastaların baskıda kırılma mukavemeti, aşınma mukavemeti gibi mekanik özellikleri, suya karşı kimyasal dayanımı ve parlatma performansını güçlendirmiştir. SiC tozunun %25'den daha fazla ilave edilmesi MOC pastaların baskıda kırılma mukavemeti ve suya karşı kimyasal dayanımında azalmaya sebep olduğu görülmüştür. Aşındırma pabuçlarının parlatma performansı parlatma testi sonunda seramik karo yüzeyinin pürüzlülüğü ve harcanan aşındırıcı miktarına bağlı olarak belirlendi. Seramik karo yüzeylerinde yapılan Taramalı Elektron Mikroskobu incelemeleri ağırlıkça %25 oranda SiC tozu ilave edilen pabuçların aşınma direnci ve parlatma performansı bakımından en üstün olduklarına dair kanıtlar ortaya çıkarmıştır.

Anahtar Kelimeler: Parlatma, Granit, Seramik Karo, Sorel Çimento, Magnezyum Oksiklorit, Aşındırcı, Pürüzlülük.

To my

Mum & Dad

ACKNOWLEDGMENTS

It is a great pleasure to thank my supervisor Prof. Dr. Abdullah Öztürk for his scientific guidance, patient supervision and valuable constant encouragement at all time. I have learned to think and understand in acedemic point of view from his training. His support and tolerance helped me to accomplish my thesis.

I would want to acknowledge Prof. Dr. Muharrem Timuçin and each one of my committee members for imparting their knowledge and motivating me to achieve this goal.

I would like to thank to all of the staff of the Department of Metallurgical and Materials Engineering for their contributions to my thesis studies. Especially, I want to thank to my colleagues Aydın Rüşen, Metehan Erdoğan, Dr. Jongee Park for their help and supports. I am also grateful to Assoc. Prof. Dr. Özgür Yaman for his advice and guidance in conducting experimental studies of my thesis.

Present work was a part of SAN-TEZ poject entilted as "*GRE Esaslı Seramik Karoların Yüzeylerinin Parlatılmasında Kullanılabilecek Kompozit Parlatma Disklerinin Üretimi*". The project was carried out together with Kaleseramik AŞ. and supported by TUBITAK with the project number 105M140. I want to acknowledge TUBITAK and Kaleseramik AŞ. for their financial and technical supports.

Lastly, I offer sincere thanks to my mum and dad for their continuous supports and encouragements, great understanding and their endless love to achieve my goals at every stage of my life. I thank to my brothers, sister, my wife and my dear doughter. Without my family this study could not be accomplished.

TABLE OF CONTENTS

LIST OF TABLES

LIST OF FIGURES

CHAPTER 1

INTRODUCTION

Polished ceramic tiles have attracted great interest in recent years due to their superior properties in chemical, mechanical and aesthetic aspect [1-8]. Ceramic tile body consists of low amount of mullite and high amount of residual quartz as crystalline phases which are dispersed in the feldspatic glassy matrix [6, 9-11]. High glass content (> 40% by volume) and low porosity (< 0.5% by volume) are typical properties of ceramic tiles that enable them for surface treatment [6, 7, 9, 11].

Surface polishing is an expensive and critical step in production of ceramic tiles [1-3, 5, 11]. Aesthetic properties of the ceramic tiles in terms of gloss and roughness are improved so much that any method but only polishing process can achieve this level [1, 2, 6]. However, opening of the closed pores already existing in the ceramic body is an unavoidable drawback of surface polishing. Moreover, if process parameters are not applied properly surface quality of the ceramic tile decreases due to scratches, grooves, cuts and subsurface cracking and polishing cost increases due to high amount of abrasive consumption [1, 3, 6, 10].

Surface polishing of ceramic tiles is achieved in three main steps; initial leveling, grinding and fine polishing. The first step involves flattening of the tile surface by diamond abrasive tools. Second is the preparation step of the tile surface for polishing by reducing roughness. It usually consists of 8 grades (46-60-80-120-180-240-320-400) with respect to the grit number of quartz and SiC particles in the abrasive bricks. Third step is the actual polishing operation where surface gloss of

the ceramic tile is improved. In this step, 600-800-1000-1200-1400-1500-1600 grit abrasive bricks are used successively.

Most common abrasive bricks for fine polishing of ceramic tiles are magnesium oxychloride cement (MOC), also known as Sorel cement, bonded SiC composite bricks [3, 11-15]. MOC is used as a binder in the production of polishing bricks due to its high early strength, excellent abrasion resistance and good bonding ability to aggregates [14-19].

MOC is a type of hydraulic cement formed by mixing proper ratio of caustic calcined MgO powder and $MgCl_2$ solution [15-28]. Four major crystalline phases are defined for MOC according to molar ratio of $Mg(OH)_2$ to $MgCl_2$ in the chemical composition: $2Mg(OH)_2.MgCl_2.4H_2O$ (F2), $3Mg(OH)_2.MgCl_2.8H_2O$ (F3), $5Mg(OH)_2.MgCl_2.8H_2O$ (F5), and $9Mg(OH)_2.MgCl_2.H_2O$ (F9) [15-19, 24-27]. However, room temperature stable phases are only F3 and F5 among which the latter is reported to have better properties in terms of chemical durability and strength [13, 16, 18, 19, 28, 29].

High concentrations of MgO ($MgO/MgCl_2$ greater than 5) in the cement paste favors formation of F5 phase, on the other hand, low MgO concentrations leads to the formation of F3 phase [16-19, 28-30]. In addition to $MgO/MgCl_2$ molar ratio, MgO/H_2O ratio is an important aspect for mechanical and chemical properties. Low water content is favorable for strength and durability of the pastes. However; the minimum amount of water is limited by workability of the paste [15, 16]. Thus, MOC pastes with high MgO and low water content are desirable [13, 15, 18].

In spite of some investigations [3, 6, 10-19] on the formation, properties and structure of MOC and ceramic tile polishing, data on the polishing performance of abrasion and polishing bricks with respect to their chemical compositions are rare and sparse. It is necessary to conduct a research to determine and improve the polishing performance of the polishing bricks if they are to be technologically useful. Otherwise the bricks may fail during service and/or may cause the formation

of nicks, scratches, cracks etc. on the surface of the tiles. An understanding of the polishing performance of these bricks is important also for correlating the abrasion and polishing behavior with the type of abrasives used in the system. Hence, studies on polishing bricks have both scientific and practical significance.

Present study was undertaken to determine the factors affecting the production and polishing performance of fine polishing abrasive bricks and to manipulate these factors to upgrade the product quality. Effects of molar composition of binder phase, type (SiO_2 or SiC), and amount of abrasive phase on the abrasion and polishing performance were clarified and discussed in detail. H_2O /$MgCl_2$ ratio of 11/1 was held constant for all cement pastes. MgO/$MgCl_2$ molar ratio of neat cement phase was studied between the range of 6/1 – 8/1. $MgCl_2$/MgO ratio of 7/1 was kept constant for the production of SiO_2 and SiC powder added composite abrasive bricks. Two grades for grinding step (46 and 180) and three grades of polishing step (600, 1200, and 1600) were chosen for experiments. For the coarse grinding (abrasion), 46 and 180 grit size quartz powder embedded MOC bricks were used. For 600 and 1200 grades of polishing, 600 and 1200 grit size SiC powder embedded MOC bricks were used. Neat (unreinforced) MOC samples were used for 1600 grade polishing.

Particle size distribution of quartz, SiC, and MgO powders were analyzed. Crystalline phases present in the MgO powder and in the neat cement were identified by X-Ray diffraction technique. Single axis compression test and abrasion test were employed for measuring mechanical properties. Chemical durability against aqueous media (water resistance) was determined via water absorption and weight loss of samples after immersing into de-ionized water.

Microstructure development in cement matrix and surface properties of abraded and polished ceramic tiles were investigated by scanning electron microscopy. Polishing performance of polishing bricks was evaluated in terms of surface roughness of the polished ceramic tile together with weight loss of the abrasive brick occurred during polishing test.

CHAPTER 2

THEORETICAL BACKROUND AND LITERATURE REVIEW

In this chapter, initially introductory information about ceramic tiles was given. Secondly, polishing process of ceramic tiles was described. Then, features of abrasive bricks and magnesium oxychloride cement (MOC) were explained in detail. Finally, previous studies concerning the subjects were summarized. Various testing methods that were applied to ceramic tiles and cement based materials by previous investigators were also mentioned in the last part.

2.1. CERAMIC TILES

2.1.1. Types of Ceramic Tiles

Ceramic tiles are divided into two main groups as glazed and unglazed ceramic tiles. Glazed ceramic tiles, differing from the unglazed ceramic tiles, include prolonged firing of the ceramic body and glazing application. Furthermore, firing procedure and composition of glazed tiles are so adjusted that a highly crystalline body and a glassy glaze is achieved. On the other hand, unglazed ceramic tiles, also called as porcelain tiles, are produced through a fast-single firing operation and includes high amount of glassy phase which enables the tiles for surface polishing operations [4-9, 13].

2.1.2. Materials Used in the Production of Ceramic Tiles

Raw materials of ceramic tiles are mainly composed of clay, feldspar and quartz. Clay provides plasticity and is considered as a source of Al_2O_3. Feldspar is used as fluxing agent and quartz plays role for viscosity of the body during sintering and contributes to mullite formation [7]. A general compositional range for the components are 40-50 clay (kaolin), 35-45 feldspar, and 10-15 quartz by weight percentage, wt% [4].

2.1.3. Sintering of Ceramic Tiles

After mixing, batching, and pressing of raw materials, ceramic tiles are subjected to high temperature for sintering purpose. Developments in materials and production techniques of ceramic tile industry yield a single firing method for ceramic tile processing [31-33]. Main idea of this process is both reducing energy costs of sintering and improving properties of product. Raw materials composition and properties are prepared in order to get a glassy matrix and mullite crystal formation at elevated temperatures such as 1200 ºC within an hour [4, 9, 13].

Firing duration cold-to-cold is usually applied about 1 h. Because of the high temperature and short firing period, ceramic tile sintering process is described as a non-equilibrium process. Dissolution of chemical components, formation of mullite crystals and glassy matrix development are kinetically controlled processes [4].

2.1.4. Structure and Properties of Ceramic Tiles

Chemical, mechanical and aesthetic properties of ceramic tiles are eminent [1-7]. They are composed of high amount of glassy phase, in-situ formed mullite crystals and residual quartz phase. Mullite crystals are generally reported as 7-8 wt% of the body, glassy matrix constitutes more than 40 wt% and the rest is typically composed of quartz. A vital property of ceramic tiles is the low amount of porosity

which is usually below 0.5 volumetric percentage, vol% [6-11]. Low amount of porosity and high amount of glassy phase make the tiles feasible for surface treatment (polishing) processes. The polishing process multiples the aesthetic appearance of the material with adequate gloss and low roughness.

2.1.5. Applications of Ceramic Tiles

Ceramic tiles are commonly used covering materials for both indoor and outdoor applications of buildings and houses [12, 13]. Due to high gloss and smooth surfaces they exhibit easy cleaning and aesthetic appearance [1, 3, 4, 6, 11]. The interest to both as-fired and polished ceramic tiles is growing in recent years.

2.2. POLISHING OF CERAMIC TILES

For improving ceramic tiles surface properties in terms of smoothness (roughness) and gloss, they are subjected to surface polishing operation after sintering process [3, 6, 10-13]. Despite the beneficial effects on appearance of ceramic tiles, polishing process exhibits difficulties and drawbacks such as opening of closed pores, grooves and high operational costs [1-3, 10].

Surface polishing of ceramic tiles are achieved on long polishing lines from coarse grade to fine grade steps. Actually, the whole surface treatment can be classified in three parts:

In the first part, diamond discs are used for leveling of the tiles. Ceramic tile surface is highly damaged and deeply scratched. Most of the material loss from tile surface occurs on this step. The diamond discs are usually called as long-life materials to express they are used for prolonged durations [10-13].

The second step can be called as grinding operation. In order to clear deep traces of diamond discs, coarse grit size abrasive powder embedded abrasives are used in grinding step. Starting from 36 or 46 grit size toward 400 grit size abrasives are used successively in 8 to 9 steps (36-46-60-80-120-180-240-320-400). In this step, ceramic tile is prepared for the polishing step. The roughness of ceramic tile decreases drastically [3, 11].

The third step, which is the main scope of this study, includes final polishing of ceramic tile. In this step, abrasive bricks are generally produced with MOC binder and very fine SiC powder as abrasive addition to the binder [11-15]. Grit sizes of abrasives are generally in the order of 600-800-1000-1200-1400-1500-1600 in the polishing line. Excellent gloss and smoothness of tile is gained in this final polishing step. For final quality of product, this step has crucial importance not to leave any process damage on the tile surface [3, 11-15].

Ceramic tile polishing system has various operational methods for different purposes. These methods are mainly classified as “Tangential Head”, “Planetary Head” and “Fixed Head” systems [3]. However, second and third step of surface polishing are mostly applied with “Tangential Head System”. Tangential Head System includes simultaneous motions of abrasive bricks in double axis. The group of 6 to 8 abrasive bricks is mounted on a circular flange which rotates around the central axis of itself. Meanwhile the rotation of flange, every abrasive brick oscillates with a 15º on the horizontal axis of abrasive brick itself. By this way, an oscillating tangential line of the abrasive brick makes contact with the ceramic tile during polishing. Hutching et al. [3] reported a schematic representation of “Tangential Head” polishing which is given in Figure 2.1.

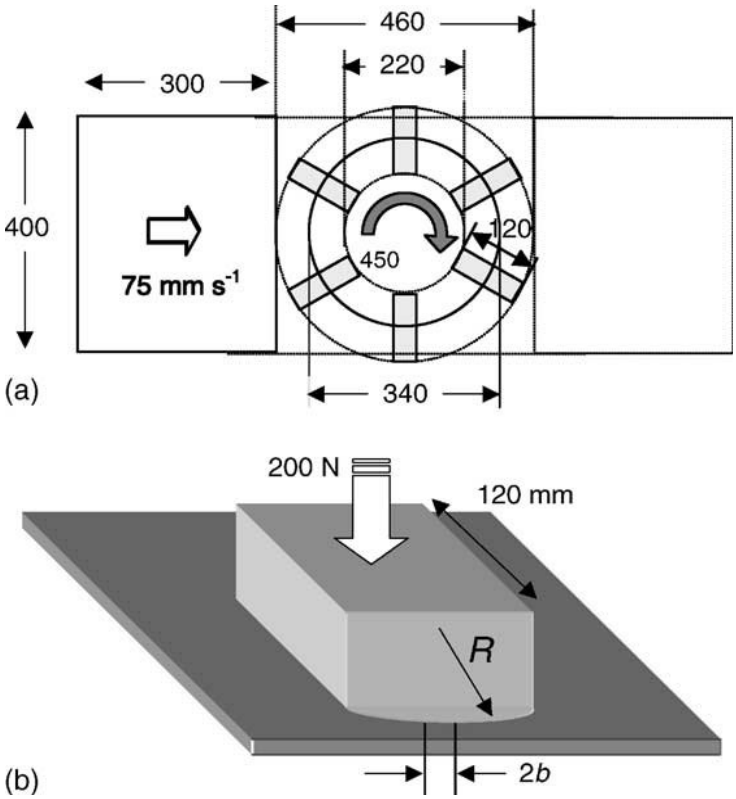

Figure 2.1. Schematic represantation of tangential head polishing. (a) A rotating head carries six abrasive blocks and the tiles are transported slowly beneath the head, (b) detail of a single abrasive block, which oscillates in a small arc with radius *R* about horizontal axis while the whole polishing head rotates about vertical axis.

2.3. MAGNESIUM OXYCHLORIDE CEMENT (MOC)

2.3.1. Materials and Formation of MOC

The MOC, also known as Sorel cement, pastes are mixtures of MgO powder and $MgCl_2$ solution in proper compositions [15-28]. Four major crystalline phases exist, defined with respect to molar ratio of $Mg(OH)_2/MgCl_2$ in the chemical composition of cement: $2Mg(OH)_2.MgCl_2.4H_2O$ (F2), $3Mg(OH)_2.MgCl_2.8H_2O$ (F3), $5Mg(OH)_2.MgCl_2.8H_2O$ (F5), and $9Mg(OH)_2.MgCl_2.H_2O$ (F9) [15-19, 24-27].

However, room temperature stable phases are only F3 and F5 among which the latter is reported to have better properties in terms of chemical durability and strength [13, 16, 18, 19, 28, 29].

High concentrations of MgO ($MgO/MgCl_2$ ratio greater than 5) in the cement paste favors formation of F5 phase, on the other hand, low MgO concentrations leads to formation of F3 phase [16-19, 28-30]. In addition to $MgO/MgCl_2$ molar ratio, MgO/H_2O ratio is an important aspect for mechanical and chemical properties. Low water content of the pastes is favorable for strength and durability. However, the amount of water is limited by workability of the paste [15, 16]. Thus, for production of polishing bricks, the MOC pastes with high MgO and low water content are desirable [13, 15, 18].

2.3.2. Properties and Applications of MOC

The MOC pastes have low thermal conductivity and good fire resistance [17]. Other than aesthetic appearance of MOC, they exhibit high compressive strength, abrasion resistance and good bonding strength to second phases like sand or gravel [13]. Due to its high performance in abrasion resistance and strength, the MOC pastes find use in abrasion brick industry [3, 13, 15]. Other uses of MOC are reported as restoration and decorative purposes [17], flooring materials in industry [24], and treatment of industrial wastes [34].

Failure of MOC due to low chemical durability against atmospheric CO_2 and moisture has been reported. Additionally, lack of resistance to weathering and leaching out of $MgCl_2$ from the cement limits the use of MOC [15, 17, 35].

2.4. ABRASIVE BRICKS FOR CERAMIC TILE POLISHING

Various types of abrasive bricks depending on type of binder material and abrasive powder were developed for polishing of ceramic tiles. Commonly used binder materials for abrasive brick applications are epoxy resin and magnesium oxychloride cement [3, 6, 10-15]. Abrasive powder choice on the other hand, depends on the quality and purpose of bricks. Namely, for coarse grinding purposes quartz and SiC particles are used together as abrasive ingredient. Pumice type porous materials are also reported to be used for more economic grinding bricks especially for marble. However, third step polishing bricks for ceramic polishing are mostly produced with only SiC powder addition to MOC [13, 14, 18].

2.5. PREVIOUS STUDIES

2.5.1. Previous Studies on Ceramic Tiles

Production procedures of unglazed ceramic tile techniques are recently developed and still being improved [1-10]. There are two important echoes of unglazed ceramic tiles to ceramic industry: reduction of production cost and improvement of product properties. Consequently, researches on the subject cover mostly material and process costs. Compositional parameters are studied to obtain possible opportunities of waste material utilization in ceramic tile production [2, 7, 36-38].

In addition to composition, effect of firing temperature is also a subject of interest. Researchers studied a certain composition of a ceramic tile body for estimating a proper firing temperature [4]. A range of 1260-1280 ºC has been stated as an optimum temperature range in terms of the amount of open and/or closed porosity, crystallization behavior and mechanical properties of the ceramic body.

Romero et al. [9] studied kinetic parameters of mullite phase formation in ceramic tiles with Differantial Thermal Analysis (DTA) and reported crystallization temperature and activation energy values for a certain ceramic tile composition. Microstructural studies have been conducted to correlate the compositional and textural properties of ceramic tiles with surface polishability [6, 10]. The investigations revealed the implications of quartz content, initial size of quartz powder and firing temperature of the ceramic tile on development of porosities.

Not only material property of ceramic tiles, but also polishing process was studied by various researchers [3, 6, 10-13]. Hutchings et al. [3] proposed a simple polishing test setup for polishing tests of ceramic tiles. The proposed system resembles to metallographic polishing method. Ceramic tile to be polished is fixed on a rotating disc and abrasive sample is held on the rotating tile. In the meantime, the abrasive sample is rotated on its vertical axis too. Consequently, double dimensional abrasion action is achieved. For the experimental polishing studies of this publication, the polishing setup designed by Hutchings et al. [3] was adopted.

Sarı et al. [39] studied polishability of various kinds of marble surfaces and defined a quantitative approach to gloss measurements of Turkish marbles. They have related the glossiness of the material with both structural properties and roughness degree. In another study on marble polishing [40], a three dimensional testing method for surface analyses was proposed. It is a kind of surface mapping system that could be used for measuring surface roughness of marble or granite tiles. The roughness range studied was mostly for coarse grinding levels such as 40 to 50 μm.

Polishing of ceramic tiles was considered as not only aesthetic but also safety aspects in various studies. Chang [41] reported the importance of friction phenomena and mentioned about occupational injuries resulting from slips and falls. A correlation between surface properties of ceramic tiles (roughness), contaminant material (water or oil) and the slipping surface (rubber sheet of shoe bottom) has been established.

2.5.2. Previous Studies on MOC

MOC or Sorel cement history goes back to 19th century when "S. T. Sorel" first invented the material which is named with the author's name in honor of him [25]. Since then, several researches have been conducted on the subject to understand and improve the properties of MOC. The first attempts identified ternary MgO-HCl-H_2O system and crystalline phase development of MOC [21]. Further researches have revealed F5 and F3 are thermodynamically and chemically stable phases at room temperature [24-27].

Dehua and Chuanmei [29] studied phase formation mechanisms in the MOC pastes and strongly stressed that crystallization of cement phase does not occur directly upon MgO and $MgCl_2$ compounds. A primary step has been described for dissolution of ionic species of Mg^{++}, Cl^-, OH^-, and H^+ in cement paste upon mixing the components. The first step was complexation of those ions into complex specie forms. They mentioned a medium gel formation and bridging reactions of complex species with the ligand H_2O and Cl^- ions. Crystallization of cement phase occurs as the result of those final bridging reactions. Studies on crystalline phases of MOC revealed that low MgO concentration in cement paste yields F3 phase formation, but; if MgO happens to exist in large amounts ($MgO/MgCl_2$ molar ratio to be more than 5/1) in the cement paste F5 phase formation is favored [18, 19, 24-26]. Microstructural examinations by Bury et al. [22] and by Dehua et al. [29] revealed that crystalline phases F3 and F5 of MOC are in elongated (needle shape) crystals.

Performance and properties of MOC were investigated by various researchers. Different compositions with different raw materials were reported for preparation of MOC pastes. Harper [23] studied the effect of calcination temperature of the magnesite for production of MOC and emphasized the importance of activity and surface area of MgO powder on the reaction kinetics and resulting mechanical properties of the cement paste. Major factors that affect properties of MOC pastes are listed as, calcination temperature and duration, powder size, porosity, surface

area and purity of MgO powder. Additionally, ratios of $MgO/MgCl_2$ and MgO/H_2O in the paste are major determinant compositional factors for the properties of MOC.

Li et al. [16] studied the effects of composition on MOC and highlighted the importance of reactivity of MgO powder. They disclosed that $MgO/MgCl_2$ molar ratio is the most critical design parameter. The mechanical tests were supplemented with X-Ray diffraction (XRD) analyses. They anticipated optimum $MgO/MgCl_2$ and $H_2O/MgCl_2$ ratios as 13 and 12, respectively for their choice of raw materials.

MOC was used as a waste treating material [42]. Refuse materials especially inorganic construction wastes were embedded in MOC to be used for outdoor floor tile production. Environmentally beneficial aspects of using urban refuse as filler material for a new product were stated.

Junsong [31] reported a foamed type material that is prepared with MOC. He mentioned the effect of phosphoric acid addition into MOC as a foaming agent. A small amount of phosphoric acid is said to be foaming the structure and covering cement crystals forming a protective layer against aqueous media. The XRD analyses revealed that cement phase formation is not affected with the addition.

Castellar et al. [15] worked on a particular case of MOC based polishing bricks. The samples of the study are reported to exhibit cracks during storage in depots. The reason of cracking was recognized as structural stress occurring due to carbonation reactions. Similar approach was applied for a case study which was about marble restorating MOC mortar [17]. The study includes XRD analyses of outdoor cement materials. The carbonation of MOC due to CO_2 gas and humidity in the atmosphere was underlined by the authors.

Present experimental study was conducted with the light of previous studies on MOC pastes, ceramic tiles, and polishing process. Understanding of production parameters for MOC based abrasive bricks and polishing process was ascertained.

CHAPTER 3

EXPERIMENTAL PROCEDURE

In this chapter, first the characteristics of the materials used for the production of magnesium oxychloride cement (MOC) based polishing bricks were given. Then, the sample preparation procedure was explained. Finally, testing methods and equipment employed in the experimental studies were described in detail.

3.1. MATERIALS

For preparation of the MOC pastes, caustic calcined MgO powder obtained from "Grecian Magnesite Co., Greece" was used. Chemical composition of MgO powder in weight percentage, wt%, is given in Table 3.1.

Table 3.1. Chemical composition of MgO powder in wt% [43].

MgO	SiO_2	CaO	Fe_2O_3
96.0	1.5	2.0	0.5

$MgCl_2.6H_2O$ salt was obtained from "Nedmag Co., Netherland" in pellet form. Chemical composition of $MgCl_2.6H_2O$ in wt% is presented in Table 3.2.

Table 3.2. Chemical composition of $MgCl_2.6H_2O$ in wt% [44].

$MgCl_2$	$CaCl_2$	Fe_2O_3	H_2O
47.0	2.0	0.2	50.8

Two grades of SiO_2 powders supplied from "Akyol TAŞ." were used for the preparation of coarse grinding abrasive bricks. Particle size of the SiO_2 powders corresponds to the grit numbers of 46 and 180. Chemical composition of the SiO_2 powders in wt% is given in Table 3.3.

Table 3.3. Chemical composition of SiO_2 powders in wt% [45].

SiO_2	Al_2O_3	Fe_2O_3	K_2O
> 98.0	< 0.6	< 1.0	< 0.4

Two grades of SiC powders supplied from Eczacıbaşı Esan AŞ. were used for preparation of composite abrasive bricks. Particle size of the SiC powders corresponds to the grit numbers of 600 and 1200. Chemical compositions of the SiC powders in wt% are given in Table 3.4.

Table 3.4. Chemical composition of the SiC powders in wt% [46].

SiC powder size	SiC	Fe_2O_3	C (Active)
600 grit	> 97.0	< 1.3	< 0.3
1200 grit	> 96.0	< 1.4	< 0.3

In addition to chemical composition, physical properties of the SiC powders given by company specifications are listed in Table 3.5.

Table 3.5. Physical properties of SiC powders [46].

Mineral Type	Crystal System	Crystal Color	Mohs Hardness
Alfa-SiC	Hexagonal	Black	9.15

3.2. PREPARATION OF ABRASIVE BRICKS

3.2.1. Equipment

Raw materials to prepare neat cement pastes and SiO_2 or SiC powders added abrasive bricks were weighed accurately (±1 g) using a Beurer KS30 model kitchen scale which had 3 kg capacity and 1 g precision.

A KitchenAid trademark "Tilt-Head Stand Mixer" with 3 lt capacity was used for mixing of the paste mixtures. The mixer had ten level of operating speed and double axis rotating paddle (KitchenAid "Flat Beater") for improved mixedness.

3.2.2. Moulds

Two sorts of home-made plastic moulds, one in cylindrical the other one in cubic shape, were used. The cylindrical moulds had a cross-section area of 8 cm^2 and height of 4 cm. Nominal dimensions of the cubic molds was 7x7x7 cm.

3.2.3. Mixing and Molding Procedure

Mixing of pastes was achieved simply in three steps: In the first step, $MgCl_2.6H_2O$ salt of required amount to obtain the molar composition of the desired paste was dissolved in water. Molar ratio of $H_2O/MgCl_2$ in the cement pastes was kept constant with 11/1 for all type of neat and composite samples. In view of the fact that there are 6 moles of chemically bonded H_2O in the $MgCl_2.6H_2O$ salt, 5 moles of extra water was added for every moles of $MgCl_2$. Salt-water mixture was blended for 10 min to dissolve Mg^{++} and Cl^- ions in the aqueous media. In the second step, the necessary amount of MgO powder was added into $MgCl_2$ solution. For SiO_2 or SiC powder embedded abrasive bricks, proper amount of SiO_2 or SiC powder was

admixed to the paste. All pastes were mixed for 30 min to obtain homogeneity and uniformity of the materials. After mixing operation, pastes were cast into moulds.

3.2.4. Compositions of Abrasive Bricks

Three different neat MOC pastes were prepared with regard to $MgO/MgCl_2$ molar ratio (6/1, 7/1 and 8/1) in the cement. The ratio of 5/1 and 9/1 were not used for the tests because the former lacked in setting reactions. The latter cracked and broken down into pieces for about 2 days after setting probably due to high amount of internal stress [13]. Molar composition of neat MOC and abrasive powder content of the bricks used in this study were presented in Table 3.6. Hereafter the samples will be referred to with the codes given in Table 3.6.

Table 3.6. Molar composition of neat MOC and abrasive powder content of the bricks used throughout this study.

Sample Code	Proportions of raw materials ($MgO:MgCl_2:H_2O$ molar ratio)	Additive grit size	SiC content (wt%)	SiO_2 content (wt%)
6-00	6 MgO : 1 $MgCl_2$: 11 H_2O	none	none	none
7-00	7 MgO : 1 $MgCl_2$: 11 H_2O	none	none	none
8-00	8 MgO : 1 $MgCl_2$: 11 H_2O	none	none	none
7-Q-46	7 MgO : 1 $MgCl_2$: 11 H_2O	46	none	none
7-Q-180	7 MgO : 1 $MgCl_2$: 11 H_2O	180	none	none
7-20- C	7 MgO : 1 $MgCl_2$: 11 H_2O	600	20	none
7-25- C	7 MgO : 1 $MgCl_2$: 11 H_2O	600	25	none
7-30- C	7 MgO : 1 $MgCl_2$: 11 H_2O	600	30	none
7-20- F	7 MgO : 1 $MgCl_2$: 11 H_2O	1200	20	none
7-25- F	7 MgO : 1 $MgCl_2$: 11 H_2O	1200	25	none
7-30- F	7 MgO : 1 $MgCl_2$:11 H_2O	1200	30	none

Molar ratio of $MgO/MgCl_2$ was 7/1 for all types of abrasive powder admixed abrasive bricks. SiO_2 powder was added only in the amount of 30 wt% for both 46 and 180 grit size. SiC powder addition was made in the amounts of 20, 25, and 30 wt% for both 600 and 1200 grit size. SiC powder embedded bricks were used in 600 and 1200 grade polishing tests. SiC addition of over 30% was not applied due to workability problems of the cement pastes.

3.2.5. Conditioning of the Samples

Neat MOC and abrasive powder embedded abrasive bricks were kept 28 days in the plastic moulds in accord with TS 1769 standard [47]. Relative humidity of conditioning room was about 50% and temperature was in the range of 20-25 ºC. After 28 days of conditioning period samples were de-molded and tested.

3.3. TESTING METHODS AND EQUIPMENT

3.3.1. Characterization

Particle size analyses of SiO_2, SiC and MgO powders were conducted using a Malvern Mastersizer 2000 model particle size analyzer. Average of three measurements for each powder sample was taken to get reliable data for particle size distribution analyses.

X-Ray diffraction (XRD) technique was applied to identify the crystalline phases present in the MgO powder and MOC pastes. Rigaku Geigerflex (DMAX/B) model X-Ray diffractometer was employed for analyses. Samples were scanned between 10º and 65º with a speed of 2 º/min using Cu-K_α radiation. Microstructure examinations of neat cement pastes and polished ceramic tile surfaces were performed by Jeol 6400 model Scanning Electron Microscope.

3.3.2. Density Determination

In determining density of the samples, the cylindrical and cubic shape samples were weighed by 1 mg precision. Density of the samples was computed by dividing the mass of the sample to volume of the sample. At least ten samples were tested for each brick to get a reliable data on density determinations. Average value of the ten determinations was calculated in g/cm^3 and taken as density of the brick.

3.3.3. Compression Test

Compression tests were performed using a compression test machine having a capacity of 300 tons (Baz Makine AŞ.). The tests were conducted at a loading speed of 240 kgf/s. Six samples in nominal dimensions of 7x7x7 cm were tested for each paste to determine the compressive strength of the bricks. Fracture load of the samples were recorded. Compressive strengths of the bricks were calculated using the formula

$$\sigma = F/A$$

where; σ represents compressive stress, F is the maximum force applied, and A is cross-sectional area of sample.

3.3.4. Abrasion Test

Abrasion tests were performed using an abrasion test machine (Atom Teknik AŞ.) in accord with TS 669 standard [48]. Three samples of bricks of each composition were involved for abrasion tests. Initial weight and height of the samples were recorded prior to the test. The test procedure basically involves erosion of bottom surface of test sample on a rotating disc by means of alumina powder laid the disc.

Nominal dimensions of abrasion test samples were 7 x 7 x 7 cm. The sample remains stationary on the disc with 20 kgf axial pressure. The abrasion of the sample occurred with the friction movement of the alumina powder between the

disc and the sample in a circular direction. A total of 22 rotations are set standard by TS 699 for a single rotation direction. After 22 rotations, the disc was stopped and test sample was removed. Disc surface was cleaned from previous dust residues. A 20 g of alumina powder was laid for every 22 rotation step. Side direction of sample was turned with 90º after each step. The test consists of 4 steps so that the erosion occurring at the bottom of the sample would be uniform in all directions. Differences of weight and height of the samples before and after abrasion test (after the whole 4 steps) were recorded to obtain the values for abrasion resistance.

3.3.5. Water Resistance

Water durability tests were carried out on ten individual samples of each paste composition. Samples were weighed and immersed in 100 ml of de-ionized water for seven days. Weight of samples was measured using a Mettler Toledo brand analytical balance (220 g capacity and 1 mg precision). After seven days duration, samples were taken out from water and freshly weighed. The difference between initial weight and weight after immersion was used as water absorption measure of the pastes. The following formula was used to calculate water absorption rate.

$$\text{Water absorption (\%wt)} = \frac{\text{(weight after immersion - initial weight)}}{\text{initial weight}} \times 100$$

After weighing, samples were dried in an oven at 65 ºC for two days to ensure all absorbed water was evaporated. After two days of drying period samples were weighed again. The difference between initial weight and dried weight was taken as the measure of the weight loss in de-ionized water.

3.3.6. Polishing Tests

3.3.6.1. Polishing Test Samples

For polishing tests, coarse ground ceramic tiles supplied from Kaleseramik AŞ. were used. Ceramic tiles were prepared in polishing facility of Kaleseramik AŞ. by grinding the upper surface with 46 grit size abrasive bricks as calibration. Also, raw ceramic tiles, which are only surface leveled with diamond disc, supplied from Kaleseramik AŞ. were used for coarse grinding tests. Nominal dimensions of ceramic tiles in length x width x depth were 30 x 30 x 1 cm, respectively.

Laboratory scale abrasive bricks for polishing performance tests were in cylindrical shape. The cross-section area of the cylinder was 8 cm^2 and height was 4 cm.

3.3.6.2. Experimental Setup for Polishing Tests

A laboratory scale polishing test setup was constructed to determine the polishing performance of the bricks. Fundamental function of the setup was to simulate industrial polishing process of ceramic tiles. The ceramic tile with nominal dimensions of 30 x 30 x 1 cm in length x width x depth, respectively, was fixed to bottom holder of the test machine. Above the ceramic tile, there were three satellites holding three cylindrical abrasive bricks each. A simple schematic drawing of the polishing test equipment is presented in Figure 3.1.

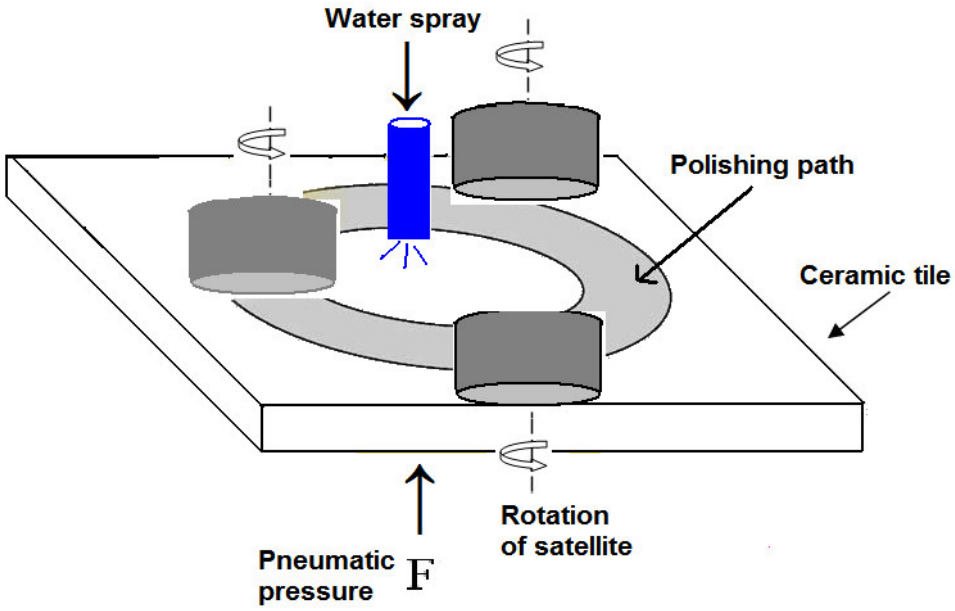

Figure 3.1. Schematic drawing of polishing test equipment.

The satellites rotated on the tile and around themselves simultaneously. By this way, three groups of three abrasives had two simultaneous motions on the tile. Tap water was pumped from the top of the machine both to cool the system and carry out the polishing sludge. Under the bottom holder of the machine, pressure was applied to the system by means of a pneumatic pump. Applied pressure and rotation speed were adjusted and set with a control panel. After the test, a circular polished path of about 5 cm wide and 15 cm outer diameter was obtained on the tile.

3.3.6.3. Polishing Test Parameters

The polishing tests were performed with the application of 2.5 bar pneumatic pressure. Rotation speed of the motor was kept constant at 500 rpm. Polishing test duration was 5 min.

3.3.6.4. Testing Procedure

Grinding (abrasion) and polishing tests were conducted in two different manners. For grinding experiments, 46 grit size SiO_2 powder embedded abrasive bricks were applied on raw ceramic tiles that were leveled by diamond disc in Kaleseramik AŞ. Surface roughness of tiles was measured using a profilometer. Initial roughness value of raw ceramic tiles was not measured because the initial surface roughness of the raw tiles was out of the measurement range of profilometer. After 46 grit size grinding, 180 grit size SiO_2 powder embedded abrasive brick was applied on the same tile. Upon completion of the grinding test, surface roughness of tiles was measured again and the results were recorded.

For polishing experiments, 46 grit size calibrated ceramic tiles supplied from Kaleseramik AŞ. were used. Surface roughness of the ceramic tile was measured before and after the polishing test. Then, 600 grade polishing test was carried out on the same ceramic tile using 600 grit SiC powder added composite abrasive brick. The data were recorded.

After the tests with 600 grade bricks, surface roughness of all ceramic tiles was brought to almost the same roughness value to get a comparable data for the second step polishing tests. In order to achieve equivalent degree of roughness, the ceramic tiles were polished with the application of 25 wt% 600 grit SiC powder added bricks for additional 5 min. Then, 1200 grade polishing tests were conducted. The data obtained after each measurement were recorded. After the second step polishing tests, ceramic tile surfaces were prepared for final polishing (1600 grade) step. Surface roughness of all ceramic tiles was brought to almost the same roughness value to get a comparable data for the final step polishing tests. In order to achieve equivalent degree of roughness, the ceramic tiles were polished with the application of 25 wt% 1200 grit SiC powder added bricks for additional 5 min. Then, 1600 grade polishing tests were conducted by the use of neat MOC bricks. The data obtained after each measurement were recorded.

3.3.6.5. Polishing Performance

3.3.6.5.1. Abrasive Consumption

The cylindrical neat MOC and composites samples (group of 9 samples for each kind of composite brick) were weighed before and after each individual polishing test. Difference between initial and final weight was considered as "weight loss" occurred during the test. The weight loss of the bricks was evaluated as "Abrasive Consumption" occurred during the 5 min of polishing test.

3.3.6.5.2. Surface Roughness

Surface roughness of the ceramic tiles was measured using a stylus profilometer (Surtronic 3+, Taylor Hobson, England) before and after polishing tests. A "TalyProfile Lite version: 3.1.4" (Taylor Hobson, England) software program was employed to trace surface profile of the polished ceramic tiles. Ten measurements were done on various locations of the polished tile to obtain reliable data. The average of ten values was taken to establish mean roughness data. Flowchart showing the experimental procedure of abrasive brick preparation is presented in Figure 3.2.

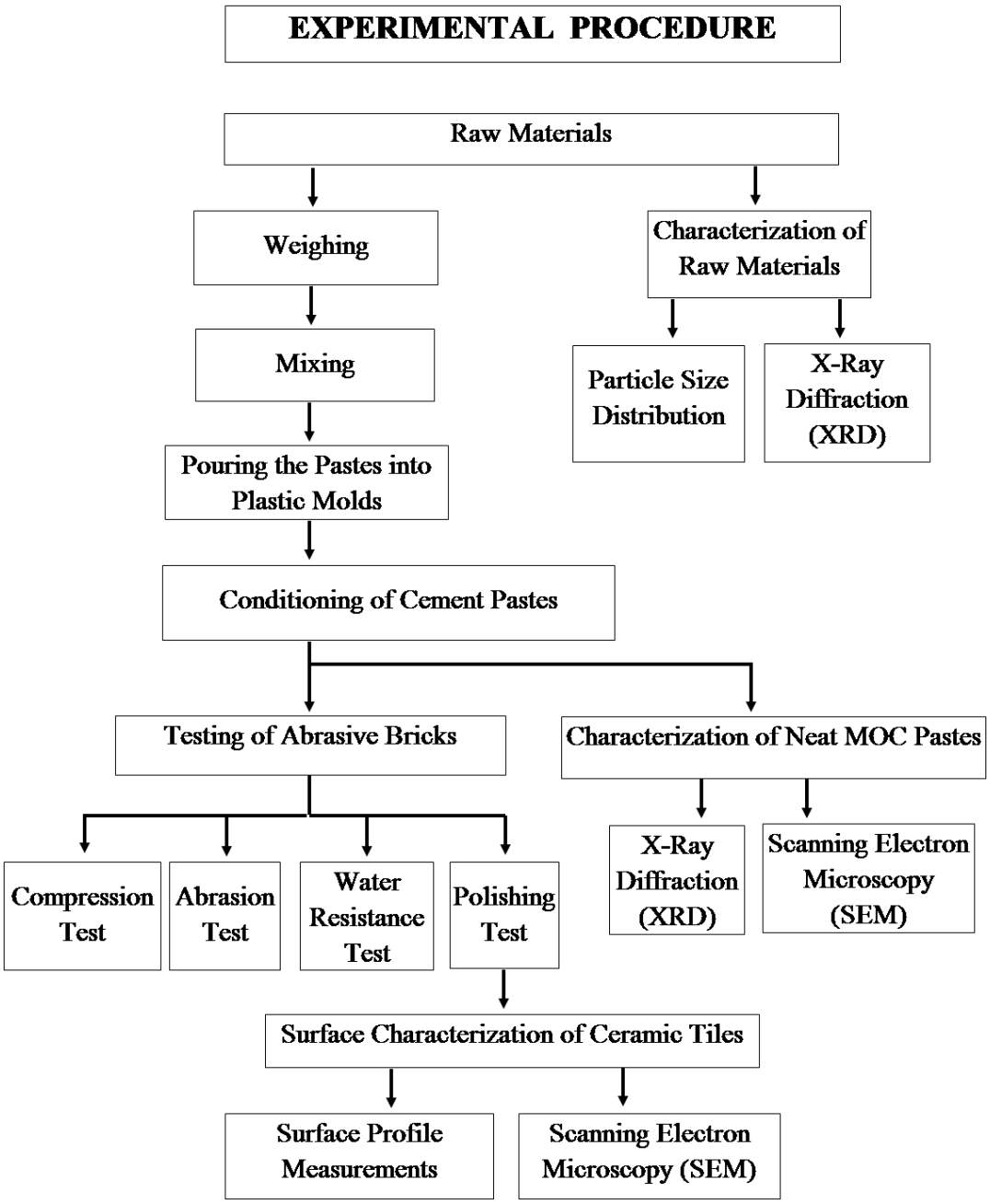

Figure 3.2. Flowchart showing the experimental procedure of abrasive brick preparation and testing.

CHAPTER 4

RESULTS AND DISCUSSION

In this section, the data gathered from the experimental study conducted on the production and characterization of magnesium oxychloride cement (MOC) based polishing bricks developed for polishing granite based ceramic tiles are presented. The MOC based abrasive grinding and polishing bricks in various compositions were formed, characterized, and tested to optimize the polishing performance of ceramic tiles. Characterization, mechanical test, durability measurement, and polishing test were performed according to the procedure as described in Section 3.3. Results obtained in this experimental study were presented, discussed and assessed with the results of the previous studies conducted on the same subject and published in the literature.

4.1. CHARACTERIZATION

Particle size distribution of 46 and 180 grit size SiO_2 powders used in the present study are illustrated in Figures 4.1 and 4.2, respectively.

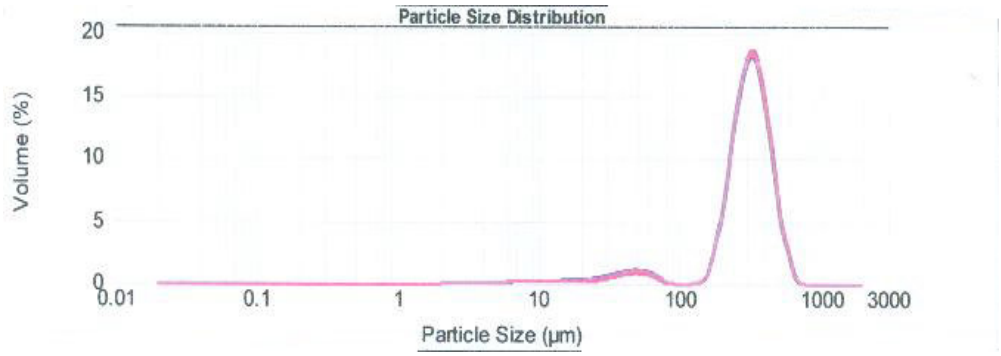

Figure 4.1. Particle size distribution of 46 grit SiO_2 powder.

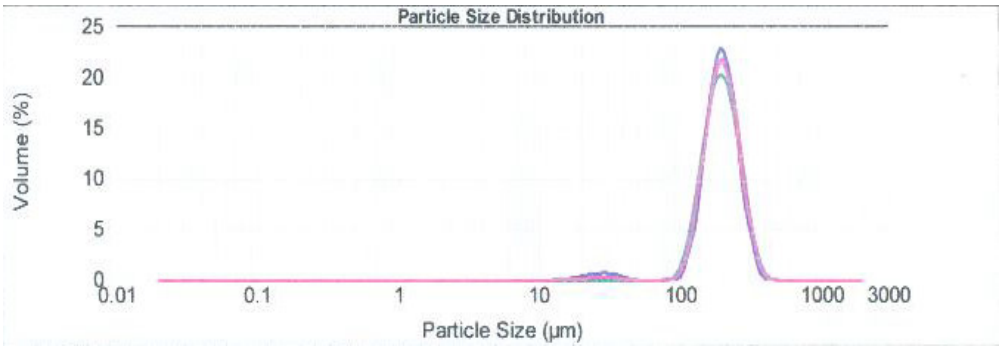

Figure 4.2. Particle size distribution of 180 grit SiO_2 powder.

Particle size distribution of 600 and 1200 grit size SiC powders are shown in Figures 4.3 and 4.4, respectively.

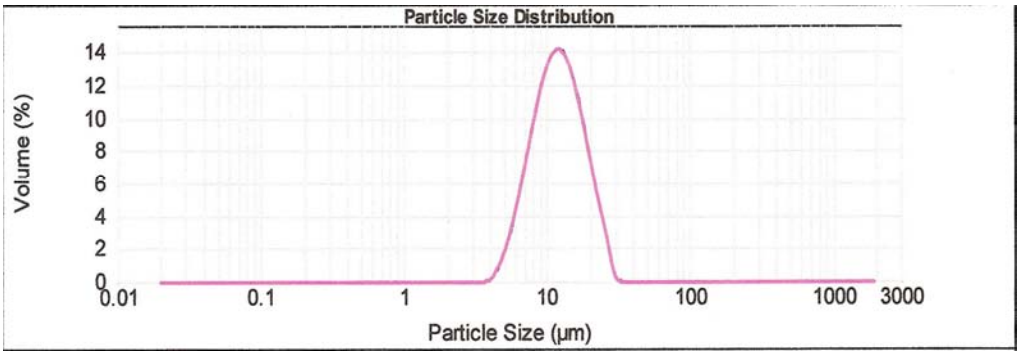

Figure 4.3. Particle size distribution of 600 grit SiC powder.

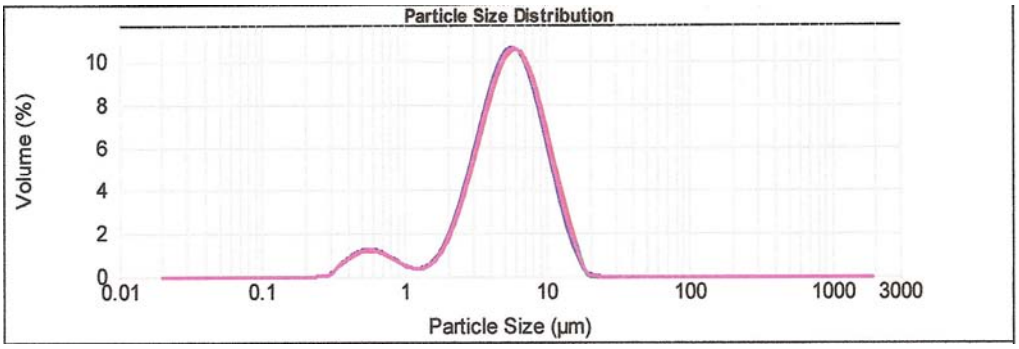

Figure 4.4. Particle size distribution of 1200 grit SiC powder.

Particle size distribution analysis of MgO powder is shown in Figure 4.5.

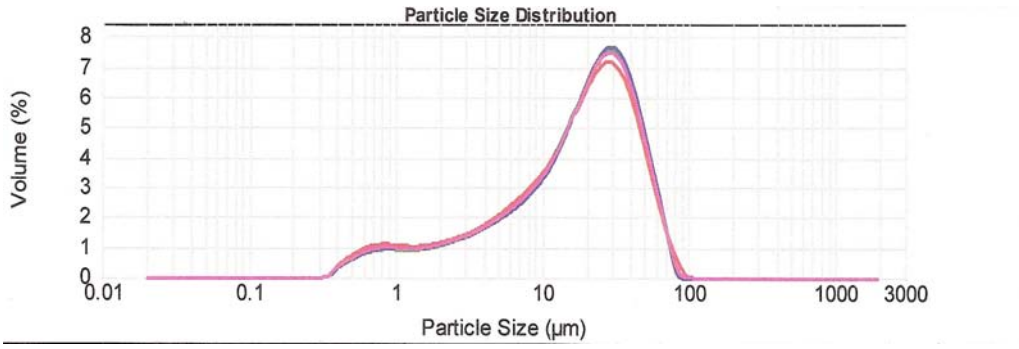

Figure 4.5. Particle size distribution of MgO powder.

Results of particle size distribution analyses of SiO_2, SiC and MgO powders are summarized in Table 4.1.

Table 4.1. Particle size distribution data of raw materials.

Grit size	d_{90} (µm)	D_{50} (µm)	D_{10} (µm)	Surface area (m^2/g)
46 (SiO_2)	456	308	179	0.034
180 (SiO_2)	276	195	136	0.064
600 (SiC)	20	12	7	0.551
1200 (SiC)	11	5	2	1.94
MgO	66	29	3	0.895

In addition to particle size distribution, surface area of the powders was measured by laser diffraction technique. Results are presented also in Table 4.1. The analyses revealed that 600 grit SiC powder had approximately four times larger surface area than 1200 grit SiC powder. The data is quite relevant with geometrical principles. That is to say, surface area is a two dimensional measure and particle size is a single dimensional (i.e., diameter) measure. Thus, surface of an object changes with square of the change occurring in particle size of the object. Surface area of MgO powder was 0.895 m^2/g, which is almost twice the surface area of 600 grit SiC powder. Large surface area of active MgO powders is reported as a result of porous structure in previous studies. Surface area and porosity are cited to be important parameters for which active MgO is dissolved in $MgCl_2$ solution but dead burnt magnesia is not [22, 23].

X-Ray diffraction (XRD) pattern of MgO powder analyzed between 2θ of 5 to 75° is given in Figure 4.6. The XRD peaks of crystalline MgO (JSPD # 45-0946) are clearly seen. Small XRD peaks for SiO_2 (JSPD # 46-1045) and $MgCO_3$ (JSPD # 86-2348) appear in the pattern. Chemical composition of MgO powder included 1.5 wt% SiO_2, which is relevant to the results of XRD analysis. A small (~ 1 wt%) amount of residual $MgCO_3$ is due to low calcination temperature of caustic magnesia [23, 30]. The XRD data obtained in this study are in accord with the results reported in the literature.

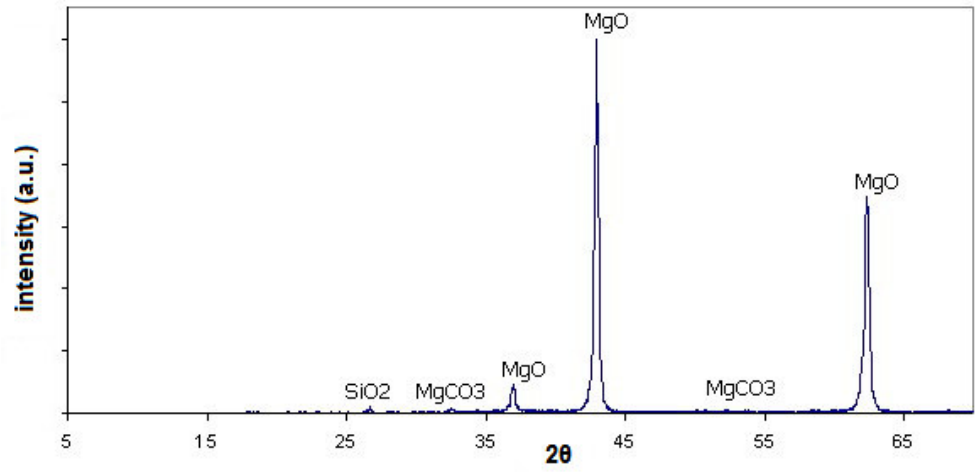

Figure 4.6. X-Ray diffraction pattern of MgO powder.

XRD patterns of the MOC pastes 6-00, 7-00, and 8-00 are given in Figure 4.7. The MOC F5 phase is indicated as F5 in the patterns. The XRD analyses of the MOC pastes revealed that all three samples essentially composed of crystalline MOC F5 phase (JSPD # 07-0420) and some amount of residual MgO. XRD patterns in Figure 4.7 exhibits two major peaks for MgO phase at 2θ of ~ 43° and ~ 62° which is the major peak of MgO. Given that the XRD pattern of MgO powder exhibited all three major peaks of MgO, the two MgO peaks in the MOC pastes is referred to as residual MgO phase in cement pastes. Formation of MOC F5 phase was favored but, formation of MOC F3 phase was not detected since the $MgO/MgCl_2$ molar ratio was more than 5. It has been reported that high concentrations of MgO ($MgO/MgCl_2$ molar ratio greater than 5) in the cement favors formation of F5 phase and low MgO concentrations leads to the formation of F3 phase [16-19, 28-30].

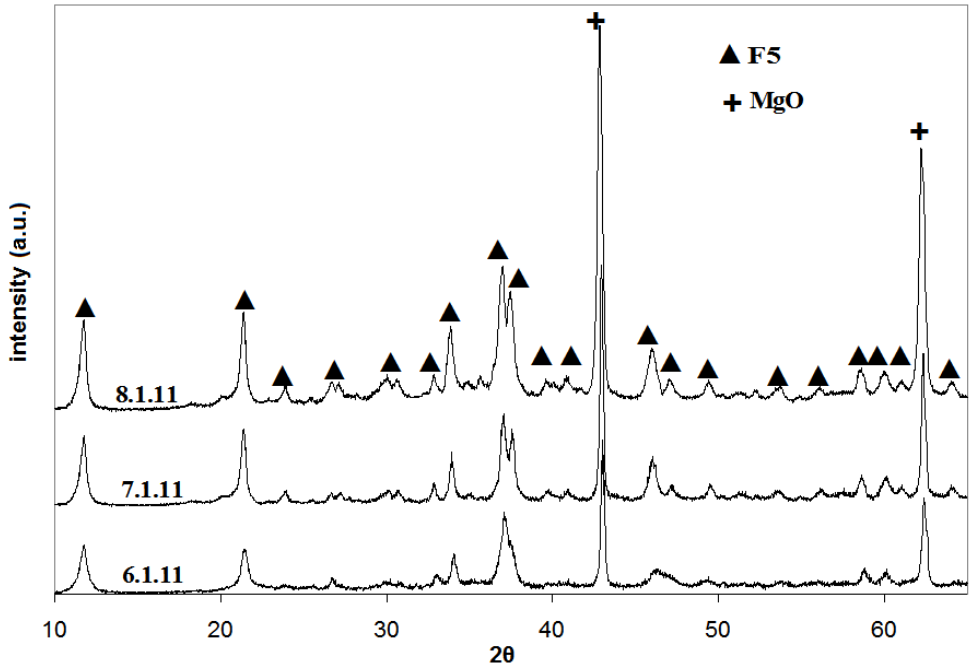

Figure 4.7. X-Ray diffraction patterns of neat MOC pastes (from bottom to top 6-00, 7-00 and 8-00). Numbers on the curves indicate the $MgO:MgCl_2:H_2O$ molar ratio.

Findings of the XRD analyses are compatible with those reported in the literature for the studies conducted on similar subjects. Li et al. [16] analyzed MOC pastes of

various molar compositions in which MgO/H_2O ratio was changed for 1 mol $MgCl_2$. Figure 4.8 illustrates XRD patterns obtained in their study. When an assessment is made between Figures 4.7 and 4.8, it is seen that the findings of this study are in good agreement with the results presented by Li et al. [16].

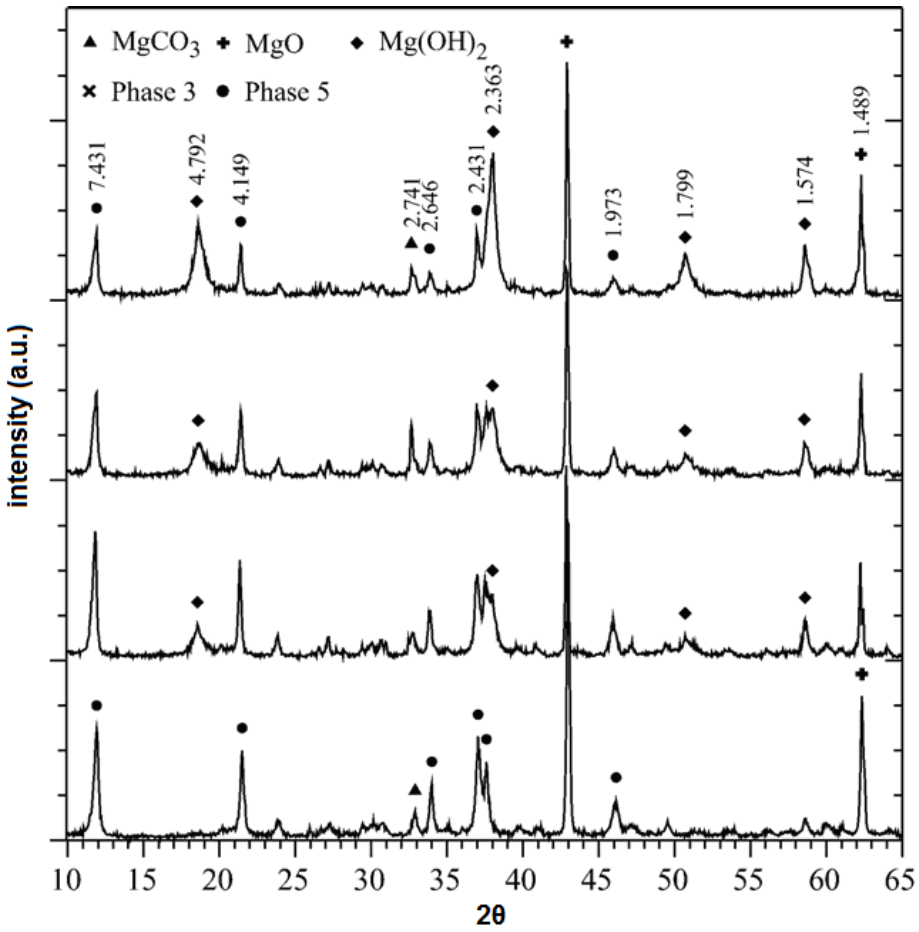

Figure 4.8. XRD patterns of MOC pastes (from bottom to top, MgO/H_2O ratio is 13/12, 13/16, 17/16, and 19/22).

Various researchers made use of intensity of XRD patterns for comparison of crystallization behavior of cementious and ceramic materials [16, 27, 34, 49]. When a comparison is made between the values of intensity of the peaks belonging to F5 phase in the MOC pastes, the intensity of F5 phase increased from paste 6-00 to paste 8-00, implying that the formation of F5 phase increased with increasing

$MgO/MgCl_2$ molar ratio in the paste. Moreover, the peaks of F5 phase sharpened with increasing $MgO/MgCl_2$ molar ratio in the paste as seen in Figure 4.7.

For the case of residual MgO phase, the comparison of XRD patterns reveals a similarity between the peak intensity values of the pastes 6-00 and 7-00. However, the XRD pattern of the paste 8-00 exhibits superior intensity peak for residual MgO as compared to the patterns for the pastes 6-00 and 7-00. The results mean that a higher amount of residual MgO phase is present in the paste 8-00.

4.2. DENSITY MEASUREMENTS

The change in density of the neat MOC pastes with regard to $MgO/MgCl_2$ molar ratio in the paste is shown in Figure 4.9. Error bars in the figure represent the ± 1 standard deviations from the average values of the determinations. It is evident that density increases continuously with increasing $MgO/MgCl_2$ molar ratio in the paste.

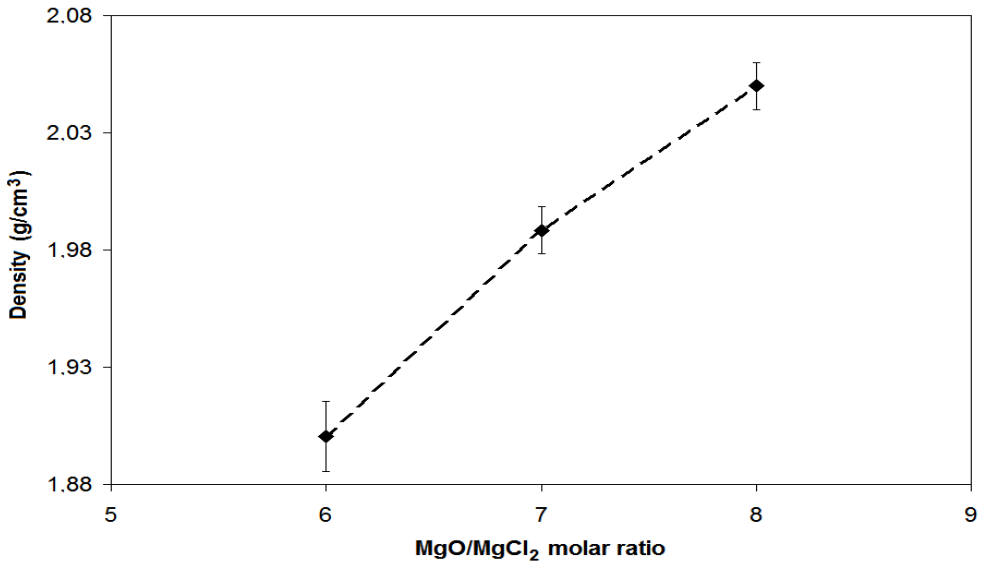

Figure 4.9. Variation in density of the neat MOC pastes with $MgO/MgCl_2$ molar ratio of the paste. The line is drawn to guide the eyes.

The density of the paste 6-00 was 1.90 g/cm^3, but increased to 2.05 when $MgO/MgCl_2$ molar ratio in the MOC paste is increased to 8. The density of the paste 7-00 which was used as binder phase in the production of abrasive bricks was 1.99 g/cm^3. The increase in density of MOC pastes with increasing $MgO/MgCl_2$ molar ratio implies that density increases also with increasing $H_2O/MgCl_2$ ratio which was kept constant at 11/1 in this study. Cement/water ratio is considered as an effective parameter on porosity and density of cement paste. Various investigators reported that density increases as cement/water ratio is increased [50-54]. Results of this study are accompanied with those reported in the literature.

The 46 and 180 grit size SiO_2 powders were added in the amount of 30 wt% to the paste 7-00 in order to prepare coarse grinding abrasive bricks. The densities of the different mixtures were compared and shown in Figure 4.10. It is obvious that density of the neat MOC paste increased with SiO_2 powder addition. However, no significant alteration in density of the 46 and 180 grit size SiO_2 powder embedded bricks was noticed. The density of both bricks was 2.09 g/cm^3.

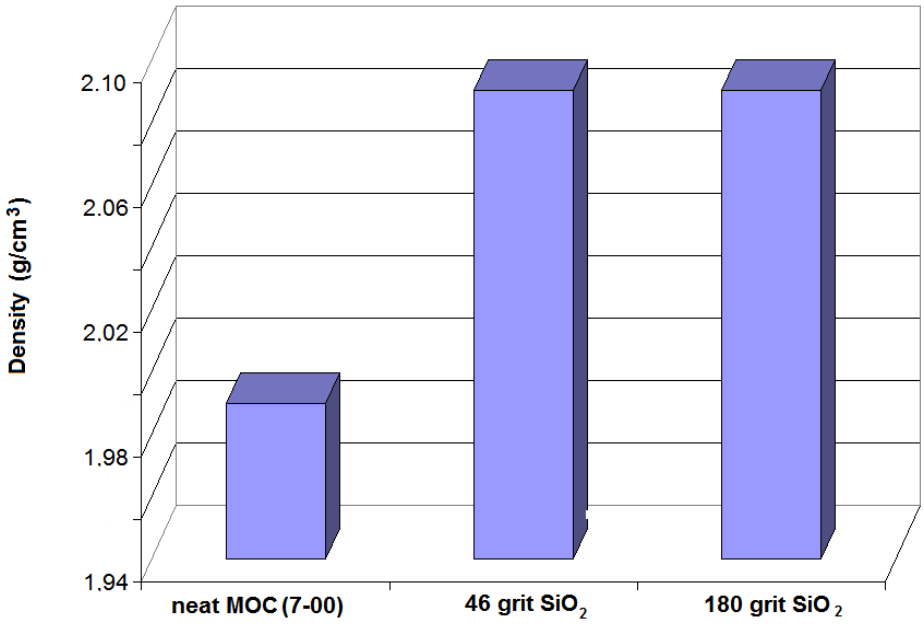

Figure 4.10. Density of different mixtures investigated in this study.

Densities of various amounts of SiC powder embedded abrasive bricks were compared with the density of the neat MOC paste. The variation in density of the 600 and 1200 grit size SiC powder embedded abrasive bricks with SiC addition is shown in Figure 4.11. Error bars in the figure represent the ± 1 standard deviations from the average values of the determinations. It is obvious that density of the neat MOC paste increased also with SiC powder additions. The density of the neat MOC paste increased from 1.99 to 2.04 g/cm^3 when 20 %wt 600 grit size SiC powder is embedded. The densities of the 25 and 30 %wt 600 grit size SiC powder embedded polishing bricks were 2.05 and 2.06 g/cm^3, respectively.

The densities of the 1200 grit size SiC powder embedded polishing bricks were not much different than those of the 600 grit size SiC powder embedded polishing bricks. The densities of the 20, 25 and 30 %wt 1200 grit size SiC powder embedded polishing bricks were 2.04, 2.05, and 2.05 g/cm^3, respectively.

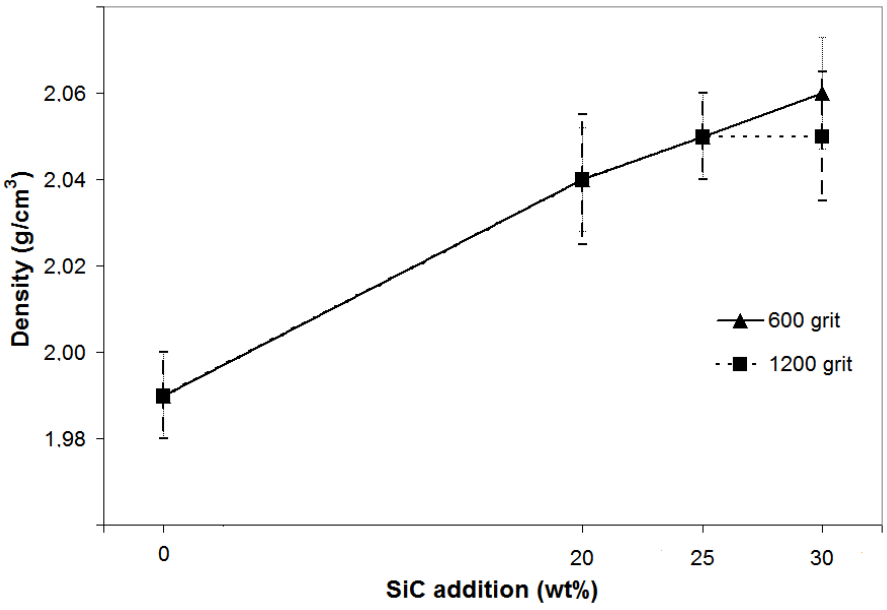

Figure 4.11. Variation in density of 600 and 1200 grit size SiC powder embedded abrasive bricks with SiC powder addition. The lines are drawn to guide the eyes.

Density measurements revealed that there is a limiting value for density of the SiC powder embedded polishing bricks. That is to say, when the SiC powder addition is increased beyond 25 wt%, further increase in density was not attained in 1200 grit size SiC powder embedded abrasive bricks. The change in 600 grit size SiC powder embedded abrasive bricks was within the error limits. This phenomenon is probably related to viscosity and porosity of cement paste. As stated earlier in Section 3.3.4, high amount of fine SiC powder additions to cement pastes decreases workability and increase viscosity [53]. High viscosity probably causes air bubbles to be entrapped in the paste but not reach the free surface. Consequently, additional SiC powder increases viscosity which in turn hinders the increase in density above a certain limit.

A similar phenomenon of viscosity is observed for a cementious material by Zhang and Han who stated that ultra-fine admixtures such as silica fume and power plant fly ash are effective on rheological properties of cement paste [55]. A low amount of ultra fine powder addition to cement paste was found to improve the rheological properties of cement paste in terms of viscosity and yield strength.

4.3. COMPRESSION TESTS

The variation in compressive strength of the neat MOC pastes with increasing $MgO/MgCl_2$ molar ratio in the paste is illustrated in Figure 4.12. Error bars in the figure represent the ± 1 standard deviations from the average values of the determinations. Compressive strength of the neat MOC pastes increased with increasing $MgO/MgCl_2$ molar ratio. The values for the compressive strength of the pastes 6-00, 7-00, and 8-00 were 53.8, 74.2, and 86.5 MPa, respectively.

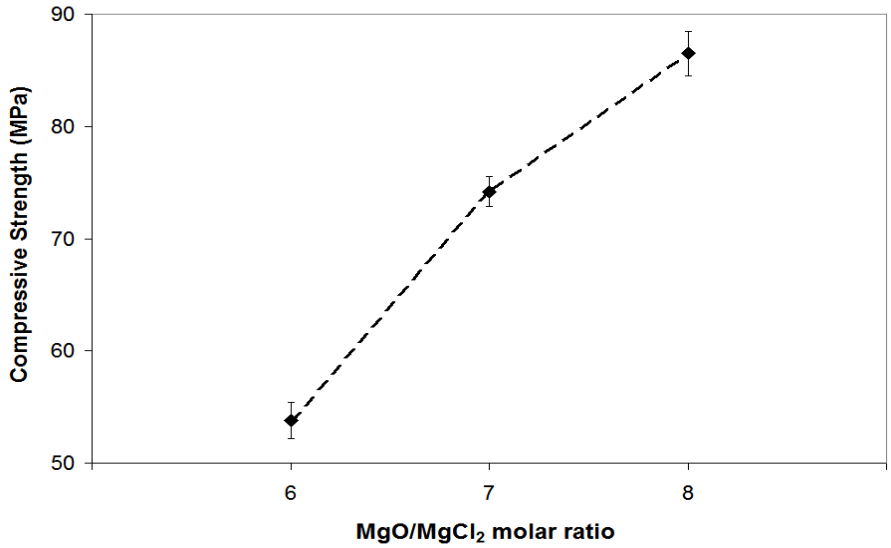

Figure 4.12. Variation in compressive strength of the MOC pastes with $MgO/MgCl_2$ molar ratio in the paste. The line is drawn to guide the eyes.

Compressive strength of MOC is widely investigated by several researchers [16, 18, 19, 23, 30, 42] who clarified two main parameters; $MgO/MgCl_2$ molar ratio and $H_2O/MgCl_2$ ratio, to be effective on strength of MOC. As $MgO/MgCl_2$ molar ratio increases, compressive strength of MOC increases. Harper [23] studied a wide range of molar compositions with three different MgO powders and found similar relation between $MgO/MgCl_2$ ratio and compressive strength. He reported 60 to 80 MPa compressive strength range for the MOC having an $MgO/MgCl_2$ ratio of 7/1. Li et al. [16] also studied compositional dependence of compressive strength of MOC. They reported compressive strength of a MOC paste with $MgO/MgCl_2$ molar ratio of 7/1 and $H_2O/MgCl_2$ ratio of 10/1 as 110 MPa. Özer et al. [56] presented 28 day-compressive strength of a MOC with $MgO/MgCl_2$ molar ratio of 7/1 as 28.8 MPa. The deviation in compressive strength of MOCs among the reported values in the literature is due to the dissimilarity in raw materials used for the preparation of MOC pastes. Indeed, various investigators stated the importance of especially MgO properties on the strength of MOC pastes [19, 23]. Calcination temperature and particle size of MgO powder were found to be among the most important factors for setting and hardening of MOC pastes.

The values of the compressive strength of SiO_2 or SiC powder embedded abrasive bricks were greater than those of the MOC pastes. Figure 4.13 presents the compressive strength values of 30 wt% 46 and 180 grit size SiO_2 powder embedded abrasive grinding bricks. Compressive strength of paste 7-00 increased from 74.2 MPa to 103.5 and 105.2 MPa with 30 wt% 46 and 180 grit SiO_2 powder addition, respectively. However, values of the compressive strength of the 46 and 180 grit size SiO_2 powder embedded bricks, were not significantly different from each other. Coarse and fine aggregate additions to MOC pastes were extensively studied by several researchers who recognized that additions of coarse and fine aggregates enhance mechanical and physical properties of MOC [54-55, 57-61].

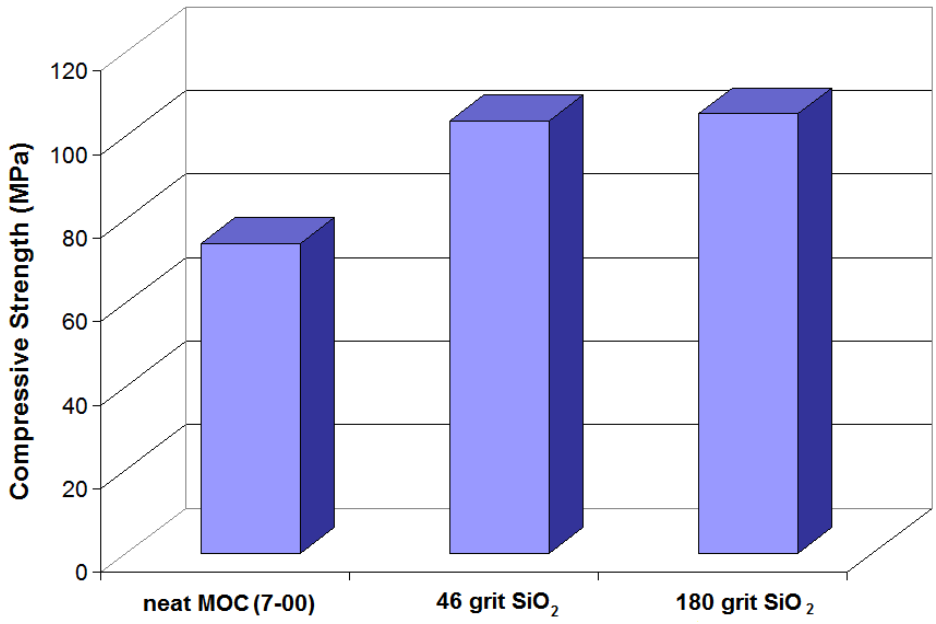

Figure 4.13. Compressive strength of different mixtures investigated in this study.

Compressive strengths of various amounts of SiC powder embedded abrasive bricks were compared with that of the paste 7-00. The variation in compressive strength of the 600 and 1200 grit size SiC powder embedded abrasive bricks with SiC powder

addition is shown in Figure 4.14. It is apparent that compressive strength of the neat MOC paste increases with increasing SiC powder additions.

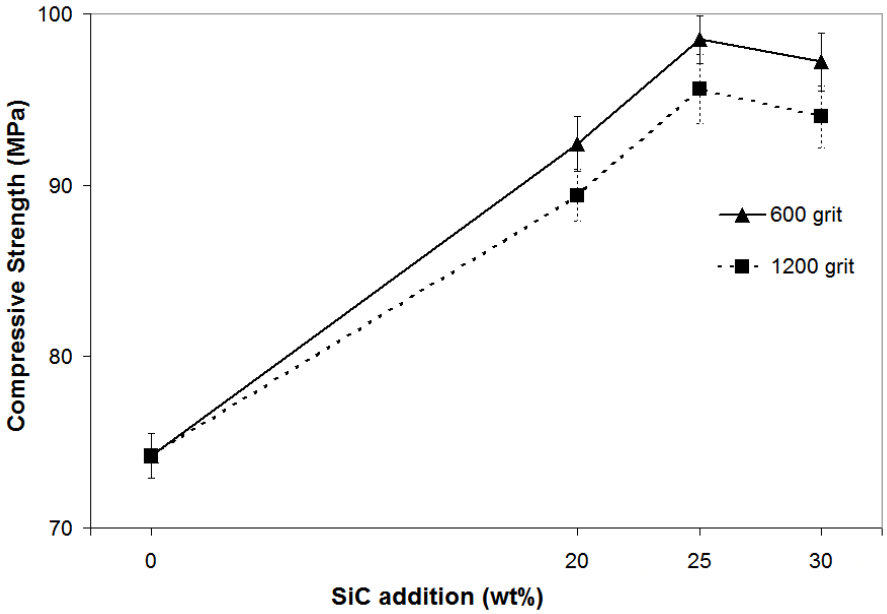

Figure 4.14. Variations in compressive strength of the 600 and 1200 grit size SiC powder embedded abrasive bricks with SiC powder addition. The lines are drawn to guide the eyes.

The compressive strength of neat MOC paste 7-00 increased from 74.2 MPa to 92.4 MPa when 20 %wt 600 grit SiC powder is embedded. The compressive strengths of the 25 and 30 %wt 600 grit SiC powder embedded polishing bricks were 98.5 MPa and 97.2 MPa, respectively. The compressive strength of the 1200 grit SiC powder embedded polishing bricks exhibited similar tendency to the 600 grit SiC powder embedded polishing bricks. Compressive strengths of the 20, 25 and 30 %wt 1200 grit SiC powder embedded polishing bricks were 89.4, 95.6, and 94.0 MPa, respectively.

Experimental results reveal that compressive strength of the MOC paste increases with both 600 and 1200 grit size SiC powder additions. The difference in the increase in compressive strength between 600 grit and 1200 grit SiC powder embedded MOCs is tied to the differences in particle size and surface area of these powder. Particle size of 600 grit SiC powder is twice the particle size of 1200 grit SiC powder. Specific surface area of 600 grit SiC powder is four times larger than that of 1200 grit SiC powder as seen in Table 4.1 in Section 4.1. Particle size and specific surface area have influence on hydration and setting reactions of cements [62]. Very fine particles of SiC powder trap more capillary water and yields microporosities in cement structure. Coarser particles of SiC powder on the other hand, contributes soundness of three dimensional MOC network by filling voids and increase compressive strength [61-63]

As seen in Figure 4.14, compressive strength values exhibited retardation over 25 wt% addition of SiC powders. Specifically, when SiC powder content is increased beyond 25 wt%, additional increase in compressive strength was not acquired due to binder/aggregate ratio is decreased. The effect of fine SiC powders on compressive strength of MOC pastes is in good agreement with the results of previous works [54, 58-60].

4.4. ABRASION TESTS

Abrasion resistance of the neat MOC pastes and SiO_2 or SiC embedded abrasive bricks was measured according to dry abrasion test as described in Section 3.3.4. Weight loss and decrease of height due to abrasion were determined and noted as test data. Figure 4.15 shows the variation of weight loss and height loss occurred during abrasion test of the neat MOC pastes as a function of $MgO/MgCl_2$ molar ratio in the paste. Error bars in the figure represent the ± 1 standard deviations from the average values of the determinations. As seen in Figure 4.15, weight loss and height loss occurred due to abrasion decreased with increasing $MgO/MgCl_2$ molar

ratio up to 7/1. Beyond that weight loss increased but height loss did not change. Weight loss occurred in the pastes 6-00, 7-00, and 8-00 was 48.6, 31.6, and 33.8 g, respectively. Height loss of paste 6-00 was 4.9 mm. Height loss occurred in pastes 7-00 and 8-00 was about the same, 3.1 mm.

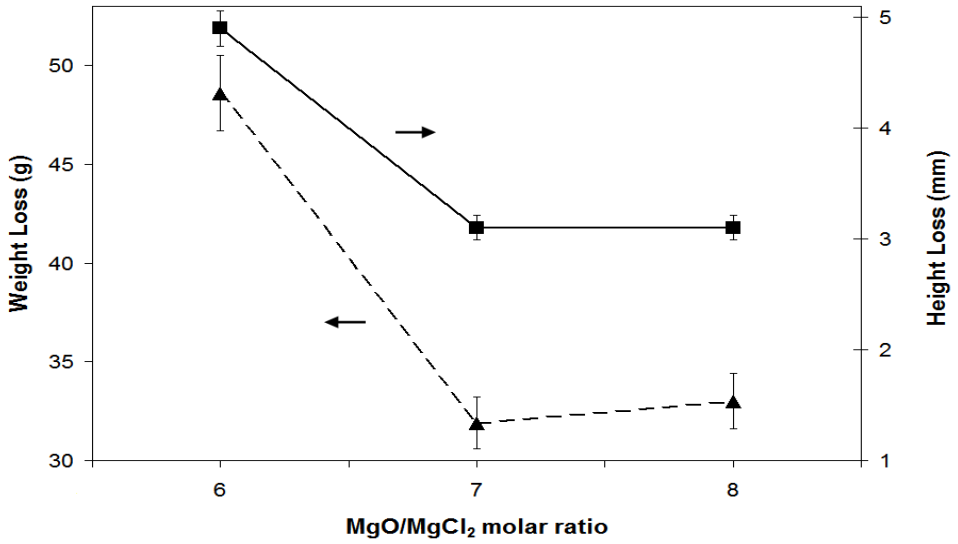

Figure 4.15. Variation in weight loss and height loss occurred during abrasion test of the neat MOC pastes with $MgO/MgCl_2$ molar ratio in the paste. The lines are drawn to guide the eyes.

Abrasion tests have revealed that abrasion resistance of the neat MOC pastes exhibit also an inflection point at $MgO/MgCl_2$ molar ratio of 7/1. When a comparison is made between the height loss values of neat MOC pastes, the paste 6-00 undergoes highest abrasion than the pastes 7-00 and 8-00. Paste 8-00 was prone to slightly higher weight loss compared to paste 7-00, although both had same height loss during abrasion tests. Indeed, the height loss of pastes 7-00 and 8-00 were small numbers and weight loss values were very close, which makes the comparison difficult. The reason why the paste 8-00 has higher abrasion than the pastes 7-00 can be attributed to the difference in density of the pastes. Since density of the paste 8-00 is greater than the paste 7-00, weight loss upon abrasion of the paste 8-00 was

measured to be greater than paste 7-00. Consequently, the paste 7-00 showed best abrasion resistance.

Abrasion resistance of SiO_2 or SiC powder embedded abrasive bricks was better than that of the MOC pastes. Figure 4.16 presents the weight loss and height loss values of 30 wt% 46 and 180 grit size SiO_2 powder embedded abrasive bricks. Weight loss value of paste 7-00 decreased from 31.6 g to 12.4 and 13.0 g with 30 wt% 46 and 180 grit SiO_2 powder addition, respectively. Height value of paste 7-00 also decreased from 3.1 mm to 1.1 and 1.2 mm with 30 wt% 46 and 180 grit SiO_2 powder addition, respectively. Addition of SiO_2 powders of both size to the MOC pastes improved abrasion resistance of MOC considerably. However, weight loss and height loss values of SiO_2 embedded abrasive grinding bricks were very close to each other. As mentioned earlier in Section 4.3, additions of coarse and fine aggregate to MOC pastes enhance mechanical and physical properties of MOC [54, 55, 57-61].

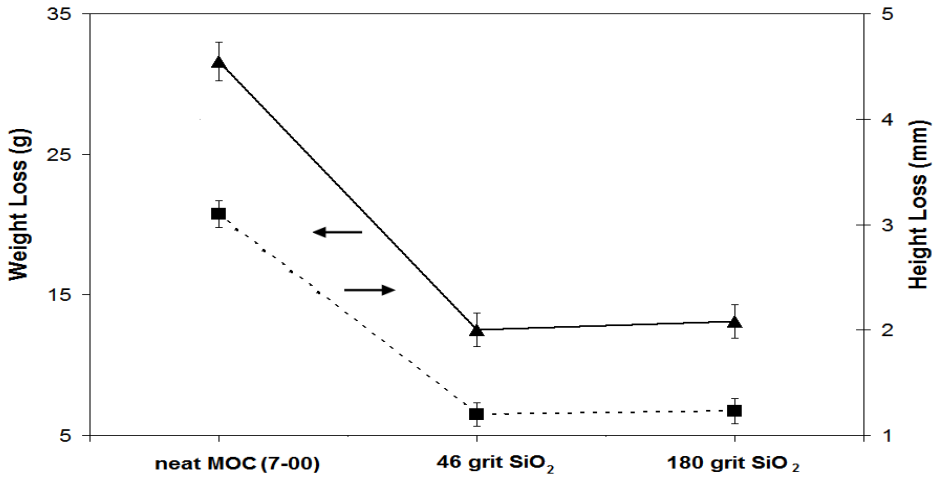

Figure 4.16. Variation in weight loss and height loss occurred during abrasion tests with SiO_2 powder addition to neat MOC. The lines are drawn to guide the eyes.

Abrasion resistances of various amounts of SiC powder embedded abrasive bricks were compared with that of the paste 7-00. The change in abrasion resistance in

terms of weight and height loss of the 600 and 1200 grit size SiC powder embedded abrasive bricks with SiC addition are given in Figures 4.17 and 4.18, respectively. It is noticeable that abrasion resistance of the neat MOC paste increases with increasing SiC powder additions.

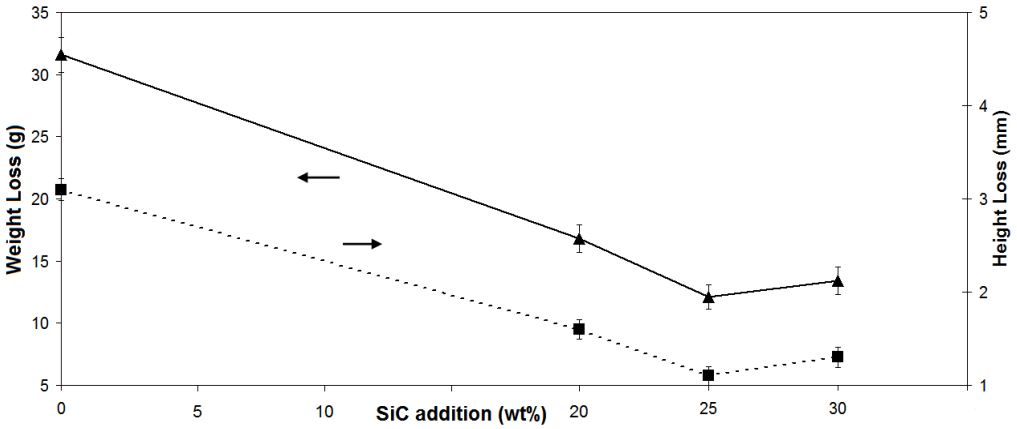

Figure 4.17. Variation of weight loss and height loss occurred during abrasion tests of the 600 grit size SiC powder embedded abrasive bricks with SiC powder addition. The lines are drawn to guide the eyes.

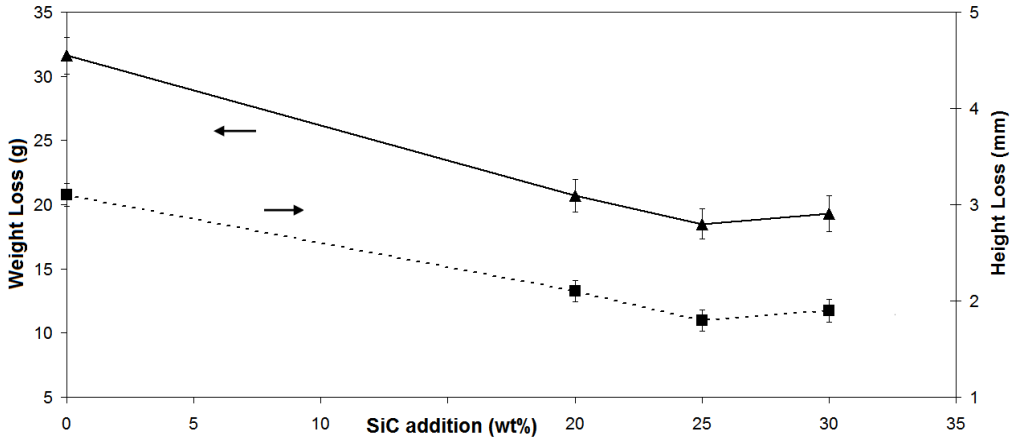

Figure 4.18. Variation of weight loss and height loss occurred during abrasion tests of the 1200 grit size SiC powder embedded abrasive bricks with SiC powder addition. The lines are drawn to guide the eyes.

Weight loss and height loss due to abrasion of paste 7-00 was 31.6 g and 3.1 mm, respectively. Weight loss of neat MOC paste 7-00 decreased from 31.6 g to 16.8 g when 20 %wt 600 grit SiC powder is admixed. Weight loss of the 25 and 30 %wt 600 grit SiC powder embedded polishing bricks was 12.1 and 13.4 g, respectively. Height loss of the 600 grit SiC powder added abrasive bricks were 1.6, 1.1 and 1.3 mm for the 20, 25 and 30 wt% SiC powder additions, respectively. The 1200 grit SiC powder embedded polishing bricks displayed similar abrasion behavior with the 600 grit SiC powder embedded polishing bricks. In the case of 1200 grit SiC powder addition to paste 7-00, weight loss values were 20.7, 18.5 and 19.3 g for the 20, 25 and 30 wt% SiC powder additions, respectively. Height loss values of the 1200 grit SiC powder embedded abrasive bricks were 2.8, 1.8 and 1.9 mm for the 20, 25 and 30 wt% SiC powder additions, respectively.

The experimental findings presented in Figures 4.15 through 4.18 reveal that abrasion resistance of MOC based abrasive bricks are profoundly affected with the three parameters: 1) $MgO/MgCl_2$ molar ratio of binder phase, 2) particle size and type of abrasive powder addition, and 3) amount of SiC powder addition. Abrasion resistance of the neat MOC pastes increased with increasing of $MgO/MgCl_2$ molar ratio, which was found to be a determinant factor on compressive strength of MOC in Section 4.3.

Unfortunately, there are only a few studies [18, 63-65] and very limited data on abrasion resistance of the MOC cements from which the results of this study could be assessed directly. However, Bauzoubaa et al. [63] reported 1.3 to 1.6 mm range of abrasion depth (which is defined as height loss in this publication) for fine aggregate embedded cements. Height loss values of the 600 grit SiC powder added abrasive bricks were within this range but that of the 1200 grit SiC powder added abrasive bricks were somehow superior. Addition of either SiO_2 or SiC powder to the MOC pastes was found to increase abrasion resistance. Figures 4.17 and 4.18 imply an inflection point for SiC powder additions. Small additions of SiC powder, such as 20 and 25 wt%, improved abrasion resistance. When SiC powder additions

were made more than 25 wt%, abrasion resistance was weaken. The decrease in the abrasion resistance with increasing amount of SiC powder is probably due to decrease in the amount of binder phase, which result in weakening of the structure. Experimental findings of abrasion tests are well-matched with those of previous works [55, 63].

4.5. WATER RESISTANCE

Water resistance of the neat MOC pastes and SiO_2 or SiC powder embedded abrasive bricks was calculated from the values obtained through measurements of water absorption and weight loss after immersion in de-ionized water for 7 days. Figure 4.19 shows the variation in water absorption and weight loss occurred during immersion test of the neat MOC pastes as a function of $MgO/MgCl_2$ molar ratio in the paste. Error bars in the figure represent the ± 1 standard deviations from the average values of the determinations.

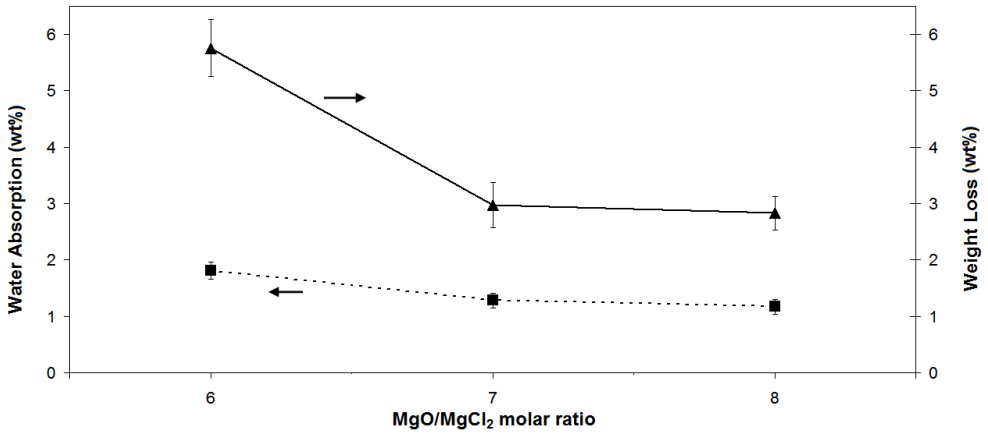

Figure 4.19. Variation in water absorption and weight loss after immersion of the neat MOC pastes with $MgO/MgCl_2$ molar ratio in the pastes. The lines are drawn to guide the eyes.

As seen in Figure 4.19, water absorption and weight loss occurred in the neat MOC pastes decreased with increasing $MgO/MgCl_2$ molar ratio up to 7/1. Beyond that water absorption and weight loss seemed unaffected with $MgO/MgCl_2$ molar ratio. Water absorption of the neat MOC pastes 6-00, 7-00 and 8-00 was 1.81, 1.28 and 1.17 wt%, respectively. Weight loss of the pastes in the previous order was 5.76, 2.97 and 2.83 wt%, respectively. Both water absorption and weight loss of neat MOC pastes upon immersion into de-ionized water decreased with increasing $MgO/MgCl_2$ molar ratio in the pastes. This is attributed to the structure developed in the MOC pastes. As the amount of MgO in the MOC paste is increased, the structure becomes more compact and less permeable to aqueous media. Also, crystallization of F5 phase, which is known with high strength and durability among the other MOC phases, is promoted with high amounts of MgO. Lastly, excess MgO in the structure of MOC serves as a blanket for protecting the F5 crystals from aqueous media [19, 29, 34]. Consequently, water resistance of MOC increases with increasing of $MgO/MgCl_2$ molar ratio.

In addition to neat MOC pastes, SiO_2 or SiC powder embedded abrasive bricks were subjected to water resistance test. Water absorption and weight loss of SiO_2 embedded abrasive bricks were calculated. Results of the water resistance test are shown graphically in Figure 4.20.

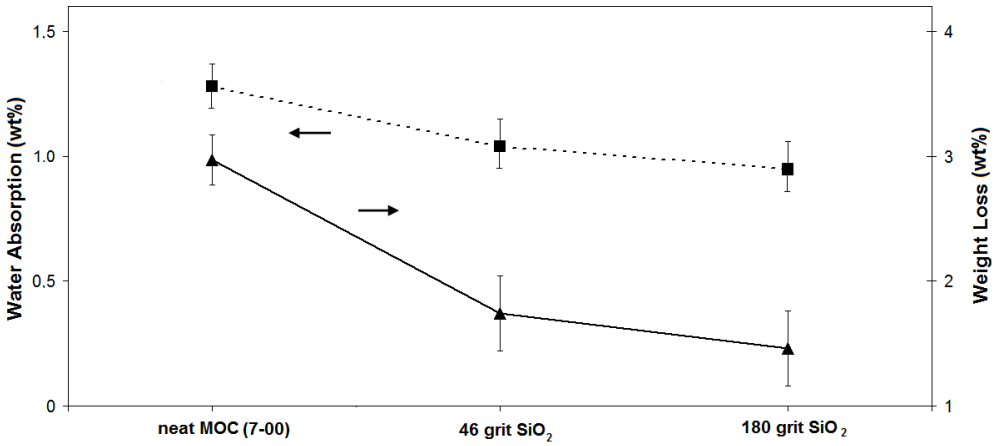

Figure 4.20. Water absorption and weight loss of different mixtures investigated in the present study. The lines are drawn to guide the eyes.

Error bars in the figure represent the ± 1 standard deviations from the average values of the determinations. Water absorption and weight loss occurred during immersion tests of the 46 grit size SiO_2 powder embedded abrasive bricks were 1.04 and 1.74 wt%, respectively. In the case for the 180 grit SiO_2 powder addition, the values were determined as 0.95 and 1.46 wt%, respectively.

Water resistance of various amounts of SiC powder embedded abrasive bricks was compared with that of the paste 7-00. The change in water resistance in terms of water absorption and weight loss in de-ionized water for the 600 and 1200 grit size SiC powder embedded abrasive bricks with SiC addition are given in Figures 4.21 and 4.22, respectively. Error bars in the figure represent the ± 1 standard deviations from the average values of the determinations. It is clearly seen that water resistance of the neat MOC paste increases with increasing SiC powder additions.

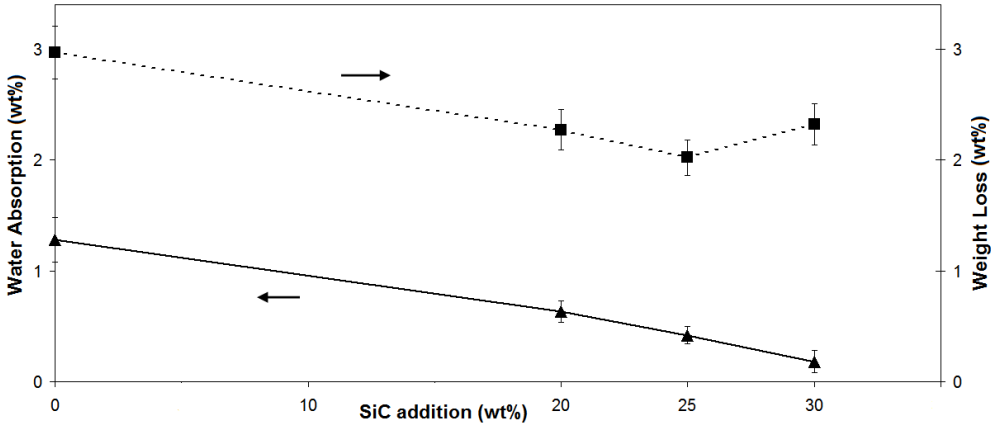

Figure 4.21. Variation in water absorption and weight loss occurred during immersion tests of the 600 grit size SiC powder embedded abrasive bricks with SiC powder addition. The lines are drawn to guide the eyes.

Water absorption and weight loss due to immersion of paste 7-00 was 1.28 and 2.97 wt%, respectively. Water absorption of neat MOC paste 7-00 decreased from 1.28 wt% to 0.63 wt% when 20 wt% 600 grit size SiC powder is added. Water absorption of the 25 and 30 %wt 600 grit size SiC powder embedded polishing

bricks was 0.42 and 0.18 wt%, respectively. Weight loss values of the 600 grit size SiC powder added abrasive bricks were 2.27, 2.02 and 2.32 wt% for the 20, 25 and 30 wt% additions, respectively.

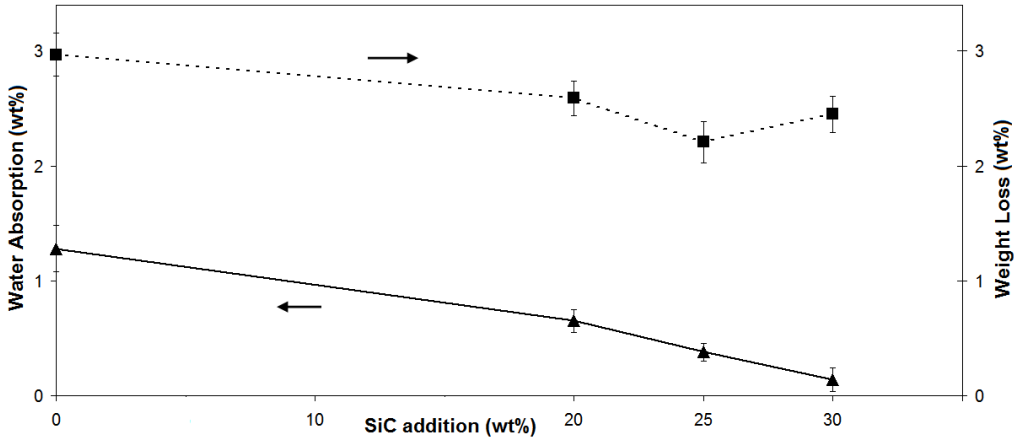

Figure 4.22. Variation in water absorption and weight loss occurred during immersion tests of the 1200 grit size SiC powder embedded abrasive bricks with SiC powder addition. The lines are drawn to guide the eyes.

The 1200 grit SiC powder embedded polishing bricks displayed similar water absorption behavior with the 600 grit SiC powder embedded polishing bricks. In the case of 1200 grit SiC powder addition to paste 7-00, water absorption values were 0.65, 0.38, and 0.14 wt% for the 20, 25 and 30 wt% SiC powder additions, respectively. Weight loss values of the 1200 grit SiC powder embedded abrasive bricks were 2.59, 2.21 and 2.45 wt% for the 20, 25 and 30 wt% SiC powder additions, respectively.

Water resistance measurements revealed that both 46 and 180 grit SiO_2 powder addition in the amount of 30 wt% improved water resistance of the MOC paste. Figures 4.21 and 4.22 illustrate an inflection point for SiC powder addition at 25 wt% where weight loss of abrasive brick increases although water absorption value decreases. The reason of inflection point is explained with the formula to calculate

the water absorption rate given in Section 3.3.5. In practice, there is an amount of mass loss which is hidden in the "weight after immersion" term due to Cl^- ion release into de-ionized water during immersion duration [17, 19, 34, 35]. Thus, the water absorption rate is not enough an accurate data on itself, however, it can be used to estimate permeability characteristics of cements [51, 58-61, 66].

4.6. POLISHING TESTS

Polishing performance of neat MOC pastes and SiO_2 or SiC powder embedded abrasive bricks was measured as described in section 3.3.6. Surface roughness of ceramic tiles and abrasive brick consumption were taken as performance parameters.

First, grinding tests were performed with the application of abrasive brick 7-Q-46 (46 grit SiO_2 powder embedded brick) on raw ceramic tiles. Upon completing the grinding process with 7-Q-46 abrasive brick, surface roughness of the tile was measured and noted. Then, abrasive brick 7-Q-180 was applied on the same tile. Upon completing the grinding process with 7-Q-180 abrasive brick, surface roughness of the tile was measured again. The data were noted and used to evaluate the grinding performance of the abrasive bricks. Mean surface roughness of ceramic tiles and abrasive erosion occurred during the application of 46 and 180 grit grinding practices are presented in Figure 4.23.

Figure 4.24 illustrates representative surface profiles of ceramic tiles upon completion of 46 and 180 grit grinding practices. Mean surface roughness of ceramic tile was 2.25 μm after the application of abrasive brick 7-Q-46 for 5 min. The consumption occurred in brick 7-Q-46 was 159.5 g. Mean surface roughness of the ceramic tile decreased to 1.39 μm after the application of abrasive brick 7-Q-180. The consumption occurred in brick 7-Q-180 was 61.8 g. When a comparison is made between the mean surface roughness and abrasive consumption

values of the abrasive bricks 7-Q-46 and 7-Q-180, erosion of the abrasive brick 7-Q-46 was almost three times greater than that of the brick 7-Q-180.

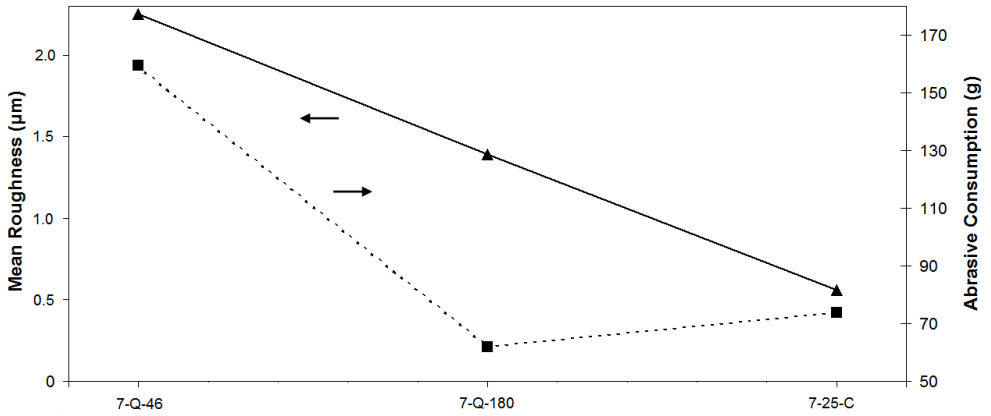

Figure 4.23. Mean surface roughness of ceramic tiles and abrasive consumption occurred during the application of 7-Q-46, 7-Q-180, and 7-25-C coded abrasive bricks. The lines are drawn to guide the eyes.

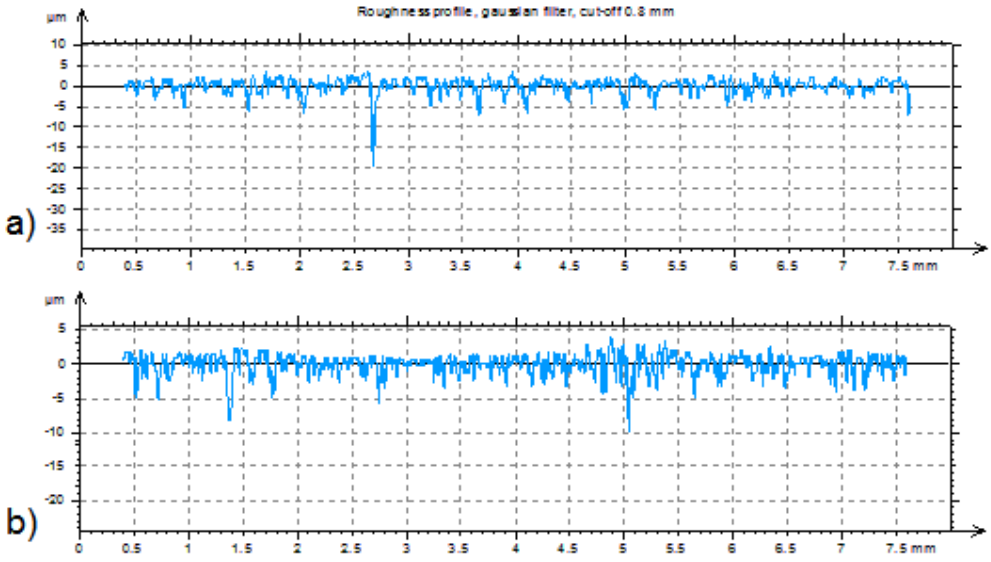

Figure 4.24. Surface roughness profile of ceramic tile after the application of abrasive bricks, a) 7-Q-46 and b) 7-Q-180.

Upon completing the grinding procedures with abrasive bricks 7-Q-46 and 7-Q-180, polishing tests were performed on 46 grit size calibrated ceramic tiles supplied from Kaleseramik AŞ. Polishing processes began with the application of 600 grit size SiC powder embedded abrasive bricks containing 20, 25 and 30 wt % SiC powder (coded as 7-20-C, 7-25-C, and 7-30-C, respectively). Then, 1200 grit size SiC powder embedded abrasive bricks containing same amounts of SiC powder (coded as 7-20-F, 7-25-F and 7-30-F, respectively) were applied on the same tile. Polishing processes ended with the application of the neat MOC paste 7-00 on the same tile. Surface roughness of ceramic tiles was measured before and after application of each bricks.

Data obtained from polishing tests were plotted in terms of surface roughness against grit number of the SiC powder embedded in the brick for different amounts of SiC powder additions. Mean surface roughness of ceramic tiles after being exposed to different polishing practices with regard to abrasive grit size is shown in Figure 4.25. The initial data point is for the mean roughness value of 46 grit calibrated raw ceramic tile supplied from Kaleseramik AŞ.

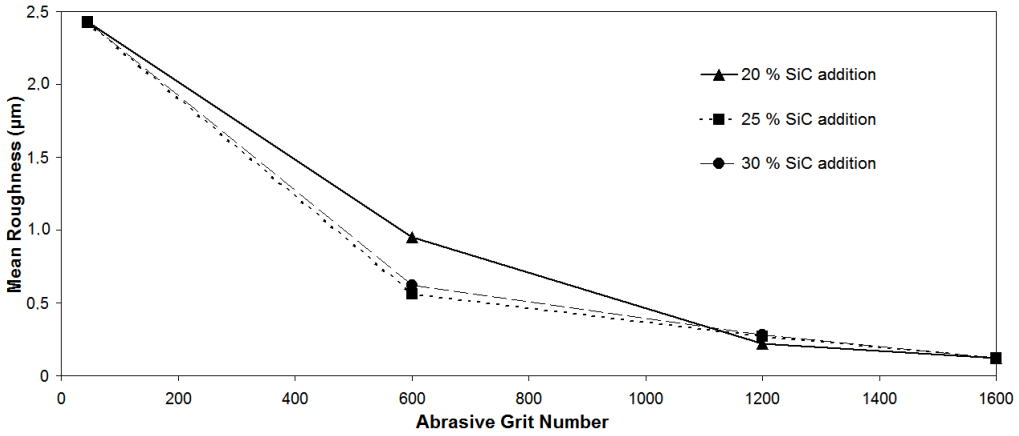

Figure 4.25. Mean surface roughness of ceramic tiles after being exposed to different polishing procedures with regard to grit size of the abrasive embedded. The lines are drawn to guide the eyes.

Mean surface roughness of ceramic tiles decreased successively in different steps of the polishing procedures. For 600 grit polishing practices, mean surface roughness of the tile was measured as 0.95, 0.56, and 0.62 µm for the bricks 7-20-C, 7-25-C, and 7-30-C, respectively. In the case of application of the 1200 grit size abrasive bricks, mean surface roughness of the tile was 0.22, 0.27, and 0.28 µm for the bricks 7-20-F, 7-25-F, and 7-30-F, respectively. Figure 4.26 illustrates representative surface profiles of ceramic tiles upon completion of 600 and 1200 grit polishing practices.

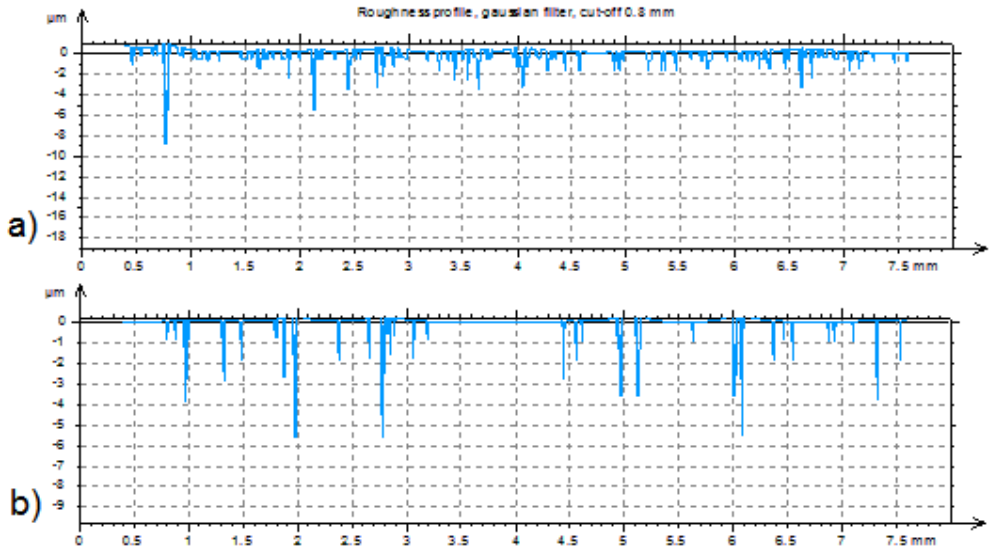

Figure 4.26. Sample roughness profile of ceramic tile after polishing with a) 7-25-C (mean roughness is 0.56 µm) and b) 7-25-F (mean roughness is 0.27 µm).

In addition to surface roughness of ceramic tiles, the consumption of the bricks during polishing practices was determined to evaluate the polishing performance of bricks. The consumption occurred in the 600 and 1200 grit size SiC powder embedded bricks are shown in Figure 4.27. Abrasive consumption occurred in the

neat cement paste 7-00 during polishing is indicated also in Figure 4.27 for comparison purpose.

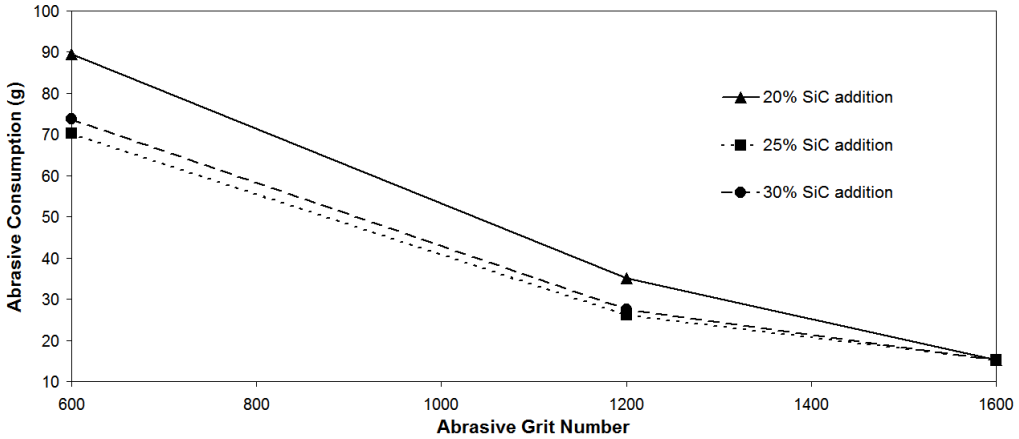

Figure 4.27. Variations in abrasive brick consumption with grit size of SiC powder for different amounts of SiC powder addition. The lines are drawn to guide the eyes.

The values of the abrasive consumption occurred in the 600 grit size SiC powder embedded bricks were 89.5, 73.8, and 70.2 g for the bricks 7-20-C, 7-25-C, and 7-30-C, respectively. As for the 1200 grit size SiC powder embedded bricks, the values of the abrasive consumption were 35.1, 27.5, and 26.2 g for the bricks 7-20-F, 7-25-F, and 7-30-F, respectively. When a comparison is made between the values of the abrasive consumption occurred in the bricks containing the same amount of SiC powder, e.g. 7-20-C and 7-20-F, it is seen that erosion occurred in the 600 grit size SiC powder embedded bricks was almost three times greater than that of the 1200 grit size SiC powder embedded bricks. In other words, erosion of abrasive bricks decreased from coarse to fine SiC powder addition. Figure 4.23 represents a similar trend for SiO_2 embedded abrasive bricks. Actually, the abrasion resistance of coarse powder embedded bricks was found to be better than fine powder embedded bricks in Section 4.3. The difference in the erosion between different grit size SiC powder embedded abrasive bricks is attributed to the initial surface roughness of the ceramic tile not abrasion resistance of the bricks [3, 14].

The initial roughness of raw ceramic tile that was leveled with diamond disc is reported to be more than 100 μm [11, 12, 14]. After the application of brick 7-Q-46, the roughness value decreased drastically implying high amount of material removal from ceramic surface [12-14]. The mean surface roughness value of the tile before the application of brick 7-Q-180 was 2.25 μm which decreased to 1.39 μm after the application of brick 7-Q-180. As a result, material removal and erosion of brick 7-Q-180 was less than those of brick 7-Q-46. Similarly, erosion in 600 grade polishing bricks was foremost among all the bricks tested, although the 600 grit size SiC powder embedded bricks were found to have greatest abrasion resistance. The reason why abrasive consumption was the foremost in 600 grade polishing practices is tied to the fact that most of the roughness reduction (smoothening) of ceramic tile surface is achieved in 600 grade polishing practice.

The aim of present study was to understand and evaluate the polishing performance of abrasive bricks. Thus, abrasive brick types should be compared for each grit size individually. For 600 grit size SiC embedded abrasive bricks, abrasive consumption of 7-20-C was the greatest, 89.5 g. Bricks 7-25-C and 7-30-C exhibited more or less the same amount of erosion (70.2 and 73.8 g, respectively) as seen in Figure 4.26. Considering the surface properties of ceramic tiles after 600 grit polishing practices, surface roughness was the greatest after exposing brick 7-20-C, 0.95 μm. Surface roughness of the bricks 7-25-C and 7-30-C were close to each other having values of 0.56 and 0.62 μm, respectively.

Polishing tests measurements revealed that among the abrasive bricks containing identical SiC powder, e.g. coarse or fine, the bricks containing 25 wt% SiC powder exhibited the best polishing performance in terms of both roughness reduction and abrasive consumption. There is very limited data reported on polishing performance of abrasive bricks with respect to abrasive composition in order to support and/or compare this judgment. Findings of polishing practices achieved in this study in terms of surface roughness and abrasive consumption values are consistent with those reported in previous publications [3, 12-14].

Three different types of neat cement pastes namely; 6-00, 7-00, and 8-00 were applied for the last step (1600 grade) polishing practices. Variation in the final surface roughness of ceramic tiles and abrasive brick consumption after 1600 grade polishing practices with $MgO/MgCl_2$ molar ratio is illustrated in Figure 4.28.

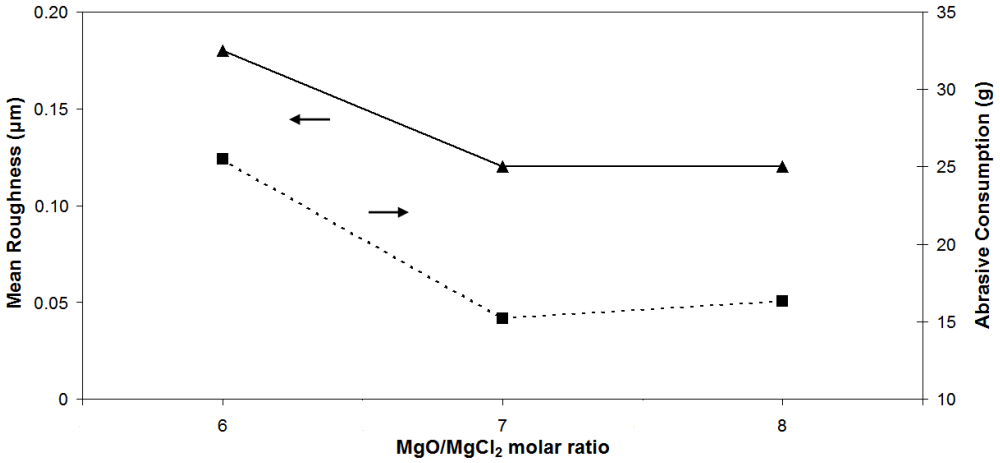

Figure 4.28. Variation in surface roughness of ceramic tile and abrasive brick consumption upon 1600 grade polishing practice with $MgO/MgCl_2$ molar ratio in the paste. The lines are drawn to guide the eyes.

Representative surface profiles of ceramic tile upon completion of 1600 grit polishing practices with the neat MOC pastes 6-00, 7-00 and 8-00 are given in Figure 4.29. Surface roughness of ceramic tile after being polished with paste 6-00 was 0.18 µm. It decreased to 0.12 µm after being polished with paste 7-00, but did not change much after being polished with paste 8-00. Abrasive brick consumption after the polishing practices was 25.5, 15.4, and 16.2 g for the pastes 6-00, 7-00, and 8-00, respectively.

Erosion of paste 6-00 due to polishing was the greatest among the neat MOC pastes. The bricks made from paste 8-00 exhibited slightly more consumption than those made from paste 7-00 although both bricks resulted in more or less the same smoothness on the tile. The reason of high abrasive consumption in paste 8-00

compared to paste 7-00 is attributed to polishing test duration [3]. Surface roughness and glossiness of the ceramic tiles on the other hand, is limited with structural and compositional properties of tile itself [6, 10, 39]. Excess of polishing durations especially for final grade (1600 grit) does not decrease surface roughness but increases abrasive consumption [3, 14, 39].

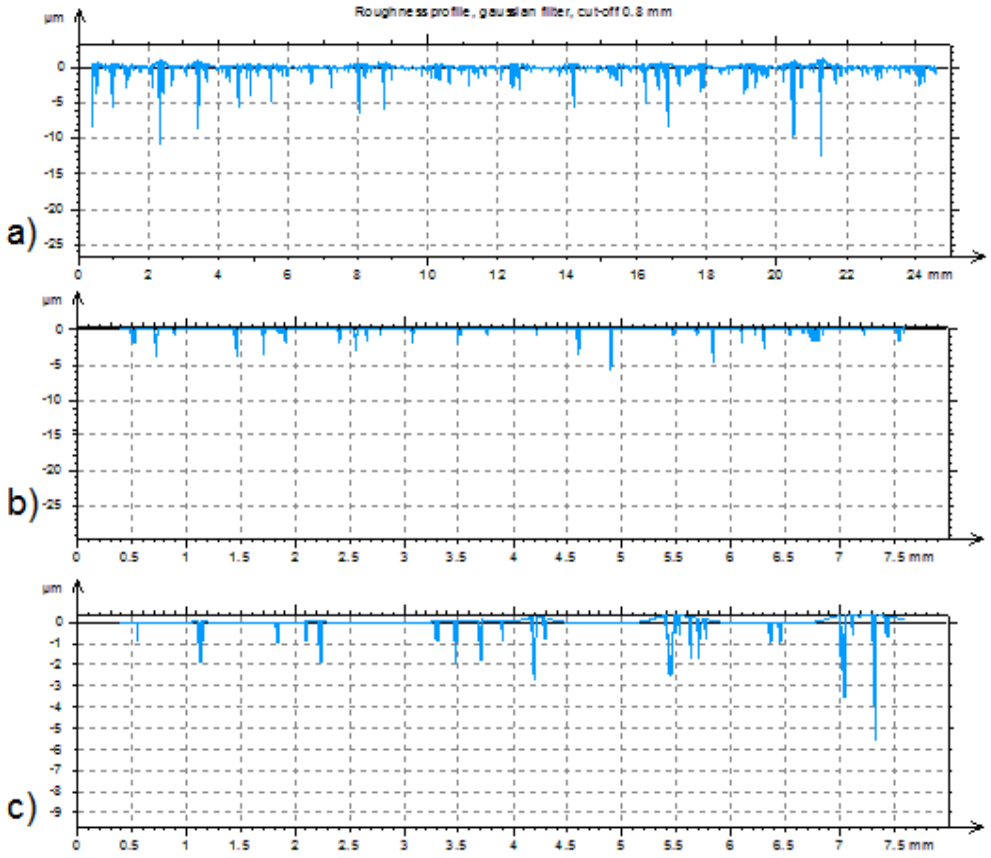

Figure 4.29. Surface roughness profile of ceramic tile after being polished with paste a) 6-00 (mean roughness is 0.18 µm), b) 7-00 (mean roughness is 0.12 µm) and c) 8-00 (mean roughness is 0.12 µm).

4.7. MICROSTRUCTURAL EXAMINATIONS

Microstructure of the neat MOC pastes and of the surface of the ceramic tiles polished with polishing disks were examined on freshly fractured or polished surfaces by Scanning Electron Microscope (SEM) according to the procedure as described in Section 3.3.1. Microstructural analyses were done to obtain supplementary information in order to evaluate the chemical and mechanical behavior observed during the tests.

4.7.1. Microstructure of the Neat MOC Pastes

A representative general view of the microstructure for the neat MOC pastes 6-00, 7-00, and 8-00 are shown in Figures 4.30 (a), (b), and (c), respectively.

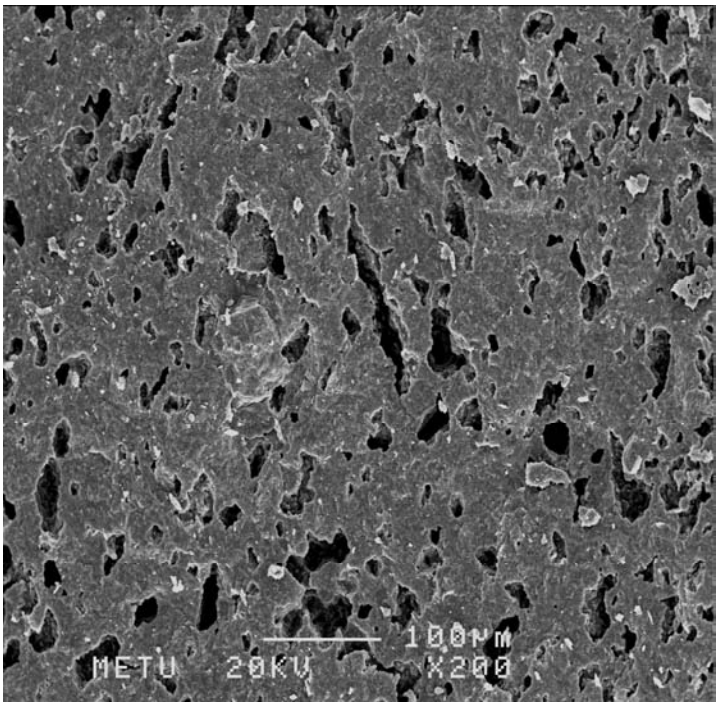

(a)

Cont…

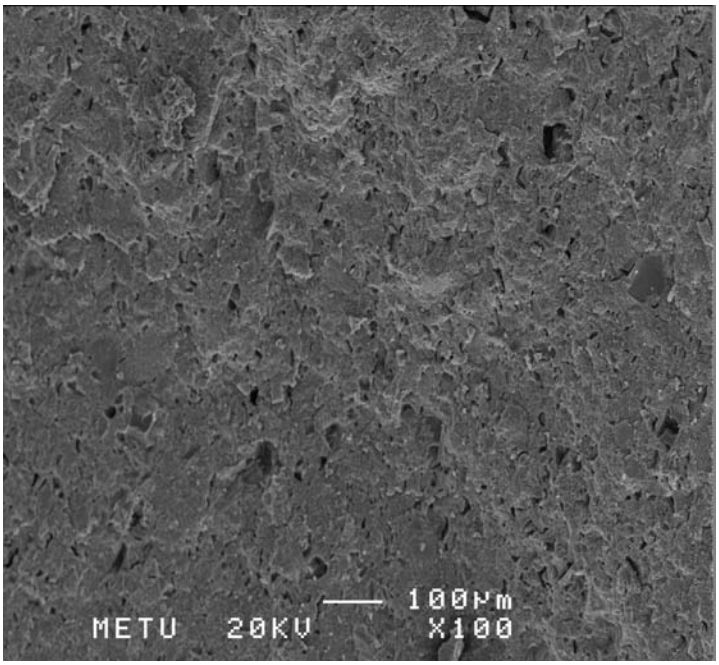

(b)

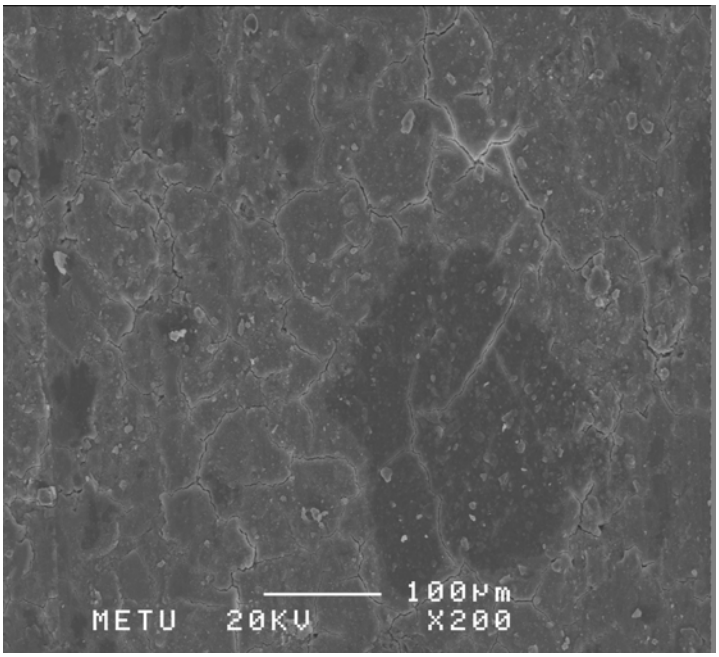

(c)

Figure 4.30. SEM fractographs of the neat MOC pastes of (a) 6-00, (b) 7-00, (c) 8-00.

SEM investigations have revealed that paste 6-00 has a porous microstructure. Micro porosities dispersed in the structure of paste 7-00 are apparent as seen in Figure 4.30 (b). Nonetheless, paste 8-00 exhibited a dense and compact structure, as indicated in 4.30 (c). The findings of the microstructure examinations are in good agreement with the density measurement and water absorption test results presented in Sections 4.2 and 4.3, correspondingly. Density is related to porosity [54, 56, 68]. As discussed earlier in Section 4.2, the density of the neat MOC pastes varies with $MgO/MgCl_2$ molar ratio. Also, the amount of water absorption of paste 6-00, which possessed least $MgO/MgCl_2$ molar ratio among the neat MOC pastes investigated, was more than that of pastes 7-00 and 8-00.

Consistent with the results given in the literature [22, 19, 29], crystalline phase development in neat MOC pastes was generally in needle shape. The needle shaped crystals were visible mostly in micro porosities of the pastes 6-00, 7-00, and 8-00 as shown in Figures 4.31 (a), (b), and (c), respectively.

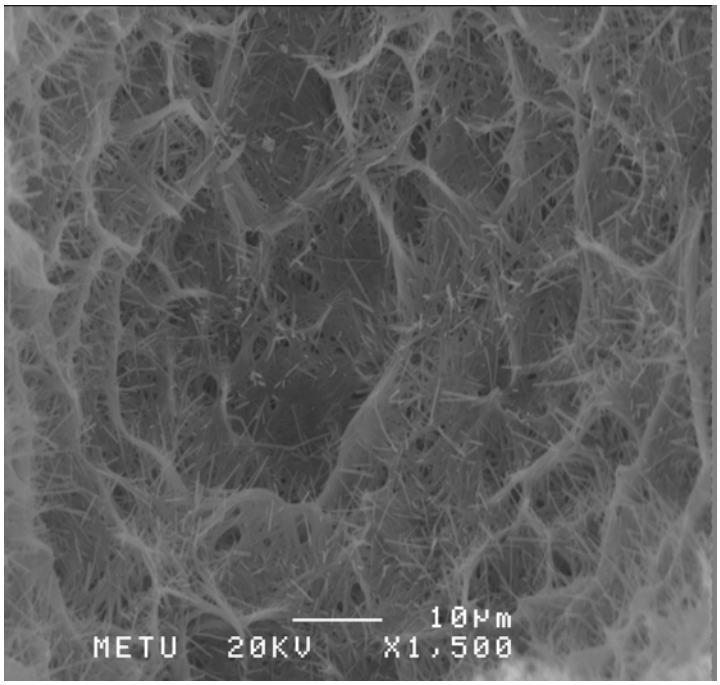

(a)

Cont…

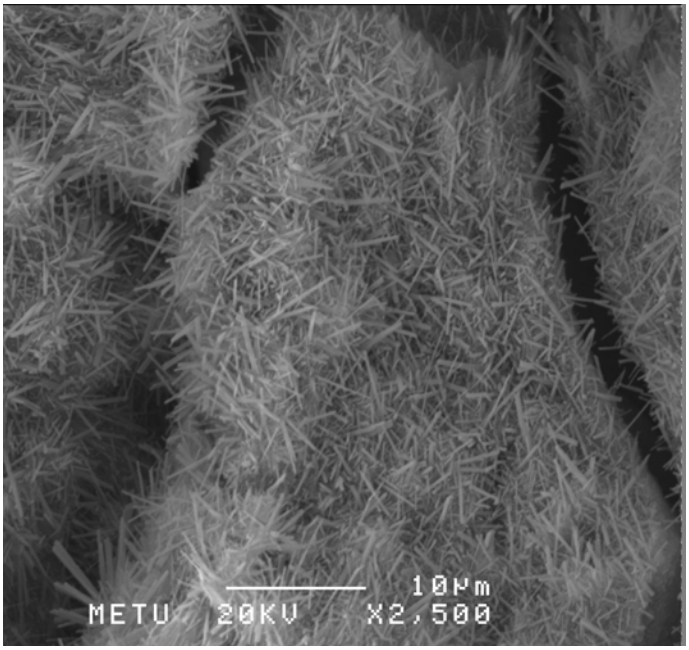

(b)

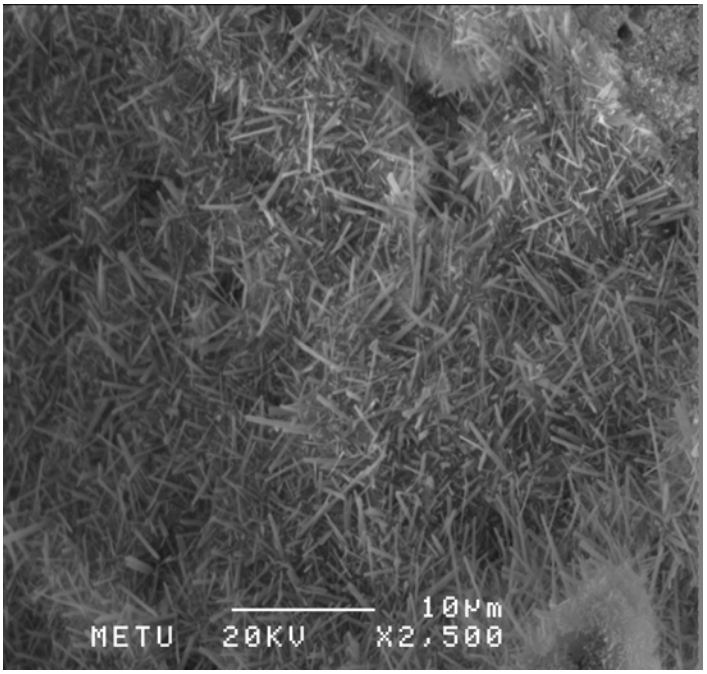

(c)

Figure 4.31. SEM micrographs of the needle shaped MOC crystals in pastes of (a) 6-00, (b) 7-00, (c) 8-00.

Porous structure of paste 6-00 is apparent in Figure 4.31 (a). The neat MOC crystals spread in loose form. Needle shaped MOC crystals are also visible in micrographs of pastes 7-00 and 8-00 as shown in Figure 4.31 (b) and (c), respectively. The needle shaped crystals were identified as MOC F5 phase in characterization studies presented in Section 4.1.

4.7.2. Surface Microstructure of Polished Ceramic Tiles

Polished surface of ceramic tiles was examined using SEM after polishing practices to determine the polishing performance of the abrasive bricks. Indeed, SEM analysis itself is not accurate enough to resolve the polishing performance of abrasive bricks, still could be used as supportive information to roughness and gloss measurements [3, 6, 10]. Therefore, microstructural observations were taken as supplementary information along with roughness measurements to understand and estimate the polishing performance of abrasive bricks. 600 grade polishing practices were applied on raw (ground with 46 grit abrasive) ceramic tiles. The abrasive bricks containing various amounts of 600 grit size SiC powder, e.g. bricks of 7-20-C, 7-25-C, and 7-30-C, were employed for this step of polishing practices. Figure 4.32 shows microstructures of ceramic tile surface after being exposed to 600 grit polishing practices with abrasive bricks containing various amounts of 600 grit size SiC powder.

SEM micrographs in Figure 4.32 exhibited the presence of open porosities on ceramic tiles. Also, scratches and polishing traces are visible in the images.

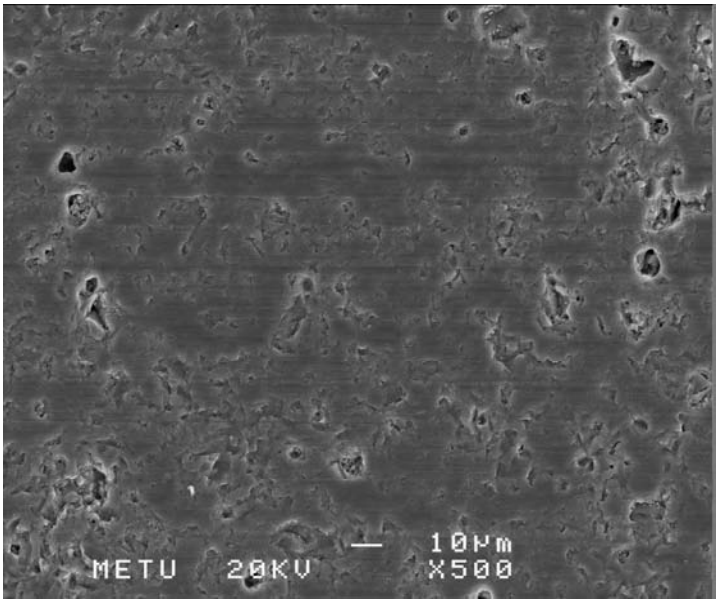

(a)

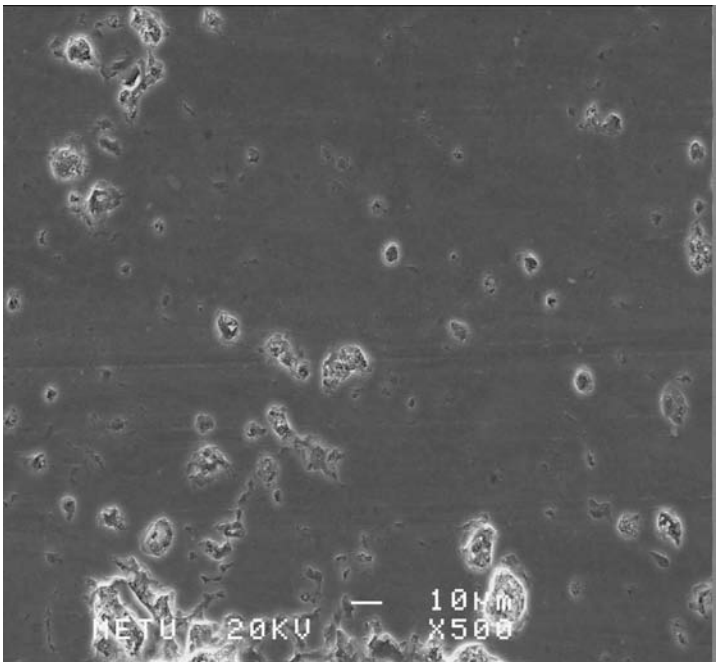

(b)

Cont…

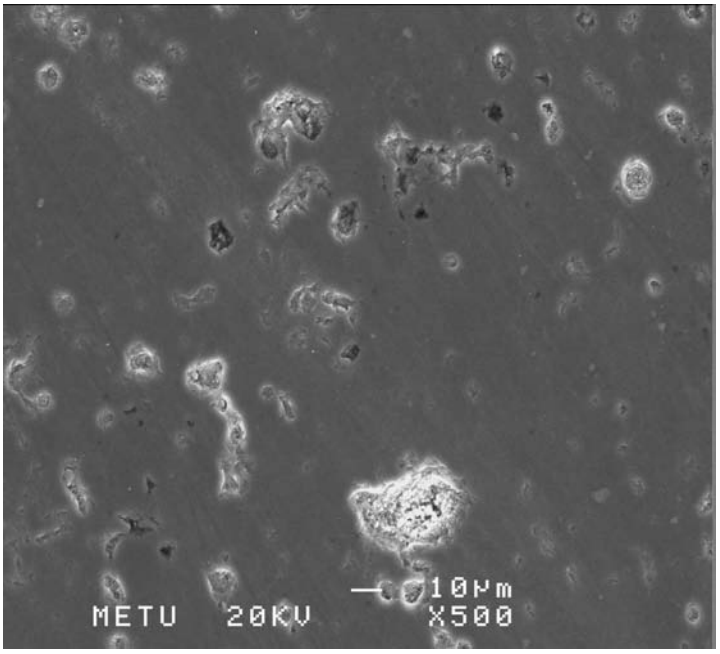

(c)

Figure 4.32. SEM micrographs of ceramic tile surface after being exposed to 600 grit polishing practice with abrasive bricks of a) 7-20-C, b) 7-25-C and c) 7-30-C.

1200 grade polishing practices were done with the application of 1200 grit size SiC powder embedded abrasive bricks. SEM micrographs taken from polished surface of ceramic tile after being exposed to abrasive bricks containing various amounts of 1200 grit size SiC powder are given in Figure 4.33. Micro porosities and polishing traces are visible in the SEM images of ceramic tiles. When a comparison is made between the images in Figure 4.32 with those in Figure 4.33, it is clear that tiles exposed to 600 grit polishing practices show evidences of more and better noticeable traces than those exposed to 1200 grit polishing practices.

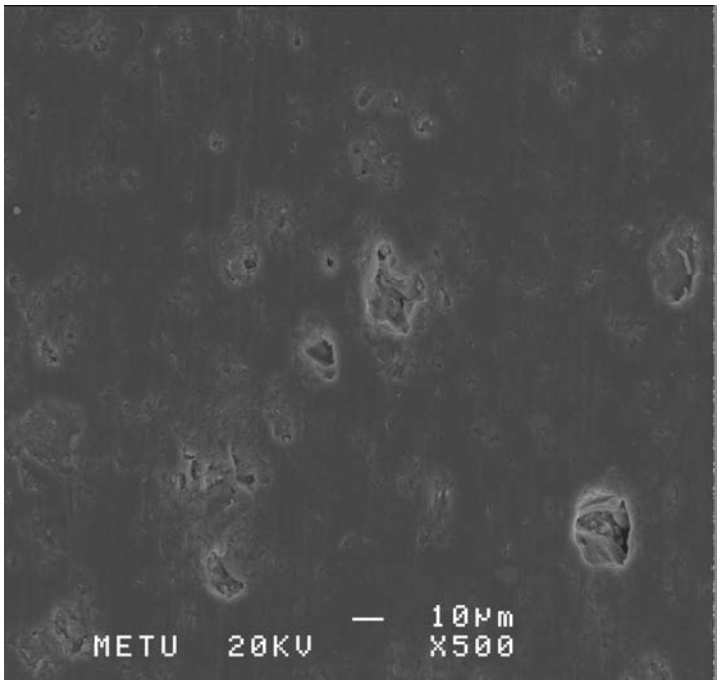

(a)

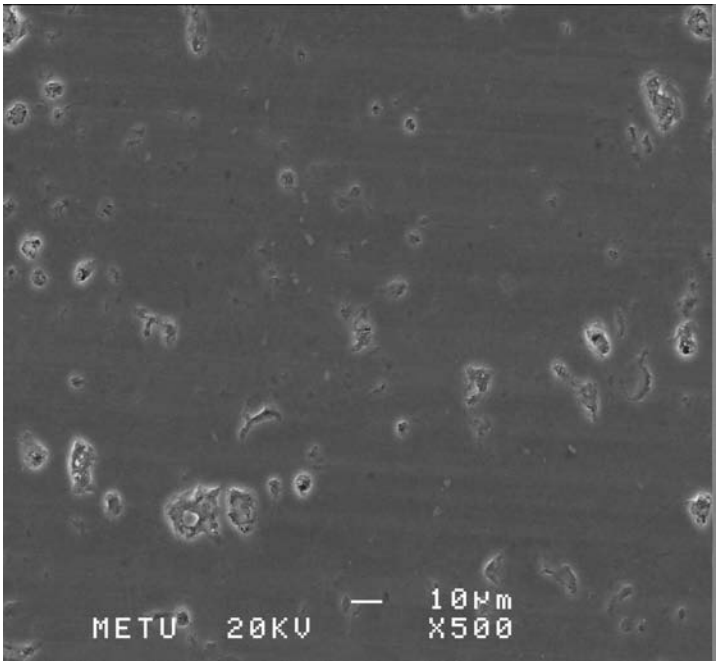

(b)

Cont…

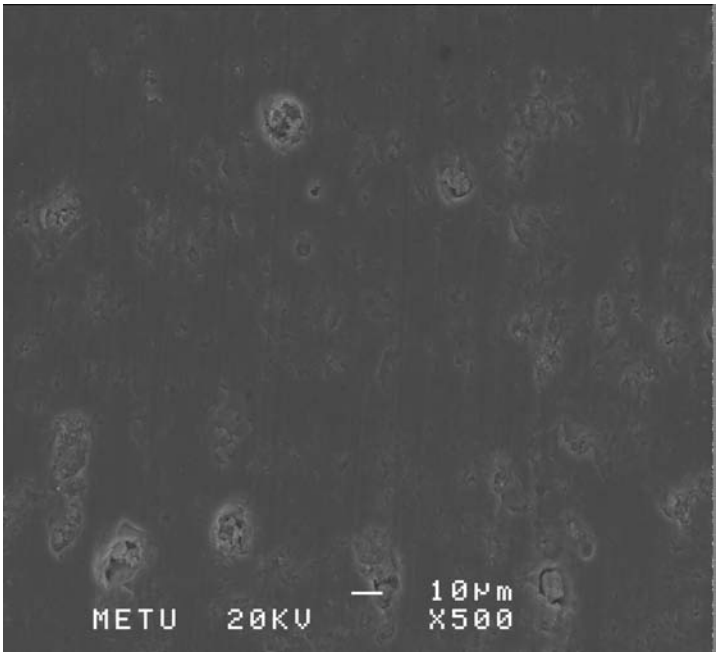

(c)

Figure 4.33. SEM micrographs taken from polished surface of ceramic tile after being exposed to 1200 grit polishing practice with abrasive bricks of a) 7-20-F, b) 7-25-F and c) 7-30-F.

SEM micrographs in Figure 4.34 show microstructures of ceramic tiles after final polishing practices with the neat MOC pastes. Figure 4.34 (b) reveals that polishing traces and scratches are removed from ceramic tile surface after polishing it with paste 7-00. However open porosities on the surface of ceramic tiles, which are intrinsic property of ceramic tiles, are evident. Esposito et al. [11] studied microstructure of polished ceramic tiles and reported plastic deformation of ceramic tile surface due to polishing process. They also mentioned opening of micro porosities in the microstructure as a drawback of polishing operation. Microstructures observed in the present work are well-suited with that observed by Esposito et al [11].

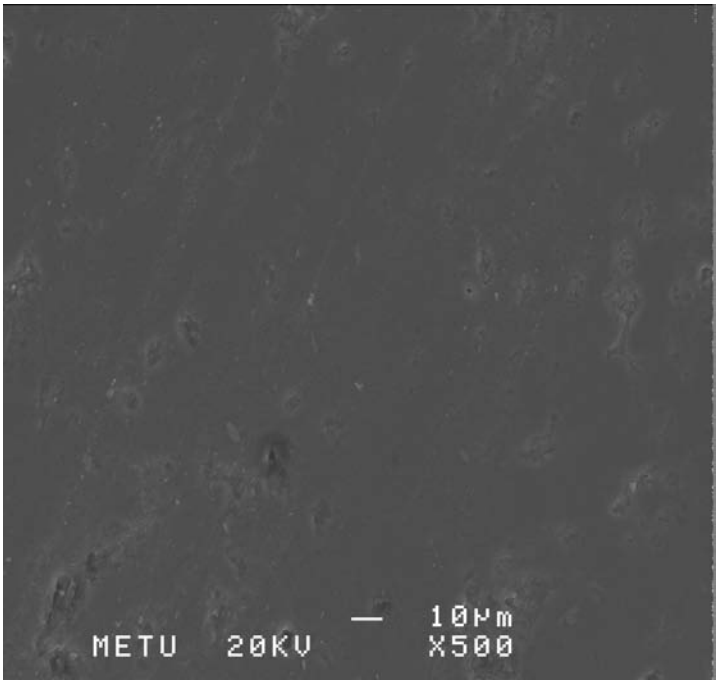

(a)

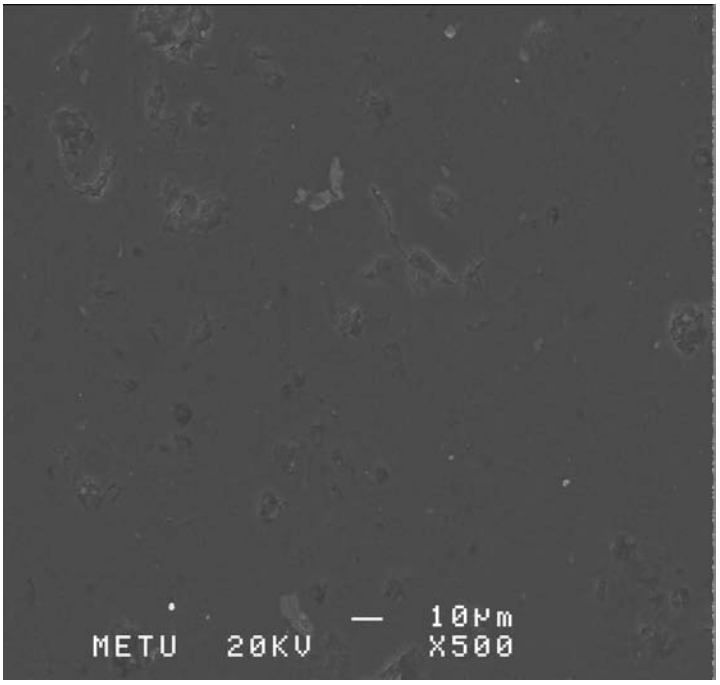

(b)

Cont…

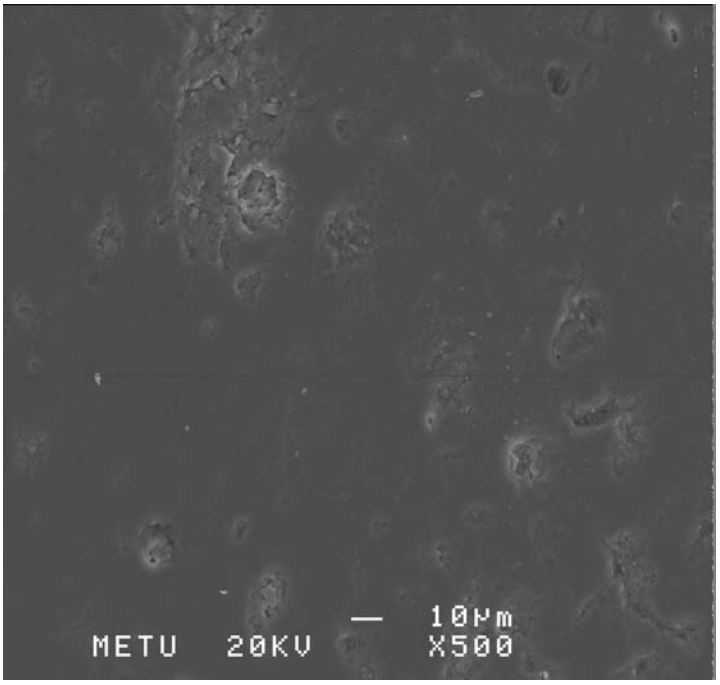

(c)

Figure 4.34 SEM micrographs taken from polished surface of ceramic tile after being exposed to the neat MOC of a) paste 6-00, b) paste 7-00 and c) paste 8-00.

Combining the results obtained from roughness measurements and SEM examinations of polished ceramic tiles, it is clear that the neat MOC paste 7-00 exhibited best qualifications in terms of polishing performance.

CHAPTER 5

SUMMARY and CONCLUSIONS

Magnesium oxychloride cement (MOC) based grinding and polishing bricks developed for polishing of granite based ceramic tiles were produced and characterized. 46 or 180 grit size SiO_2 powder embedded MOC based abrasive bricks were applied on granite ceramic tiles to accomplish surface grinding. For polishing practices 600 and 1200 grit size SiC powder embedded MOC based polishing bricks and neat (unreinforced) MOC pastes were exposed on granite ceramic tiles.

The bricks were prepared by conventional technique of mixing and molding of the cement paste. Three different neat MOC pastes depending on $MgO/MgCl_2$ molar ratio in the paste were formed. Grinding bricks were formed by adding 30 weight percentage, wt%, of both of the SiO_2 powders. Polishing bricks were formed by adding 20, 25, and 30 wt% of each SiC powders. Crystalline phase formation and microstructure of the neat cements were examined using X-Ray powder diffraction and scanning electron microscope, (SEM). Mechanical properties namely; compressive strength and abrasion resistance, chemical durability in water and polishing ability of the neat MOC pastes and abrasive bricks were determined to improve the polishing performance. Density, water resistance, and abrasion resistance of MOC paste increased with increasing $MgO/MgCl_2$ molar ratio in the paste. Improvement in water resistance was due to promotion of the formation of F5 crystals and low porous compact structure in MOC pastes.

Additions of either SiO_2 or SiC powders had a profound effect on compressive strength and water resistance of MOC pastes. Increasing additions of fine and coarse SiC powders up to 25 wt% enhanced mechanical properties. More than 25 wt% addition of SiC powders had a tendency to decrease the compressive strength and water resistance of MOC paste.

The MOC paste composed of 7:1:11 molar ratio of $MgO:MgCl_2:H_2O$ was found to have greatest resistance to abrasion. Type and amount of abrasive powder addition had a powerful effect on abrasion resistance. Additions of either SiO_2 or SiC powders improved abrasion resistance of MOC paste, too. Advancement in the abrasion resistance of MOC with 30 wt% 46 or 180 grit size SiO_2 powders addition was more or less the same. Additions of 600 or 1200 grit size SiC powders up to a limiting value of 25 wt% led to an improving effect on abrasion resistance. For a given amount of addition, coarse SiC powders were more effective than fine SiC powders.

Polishing performance of abrasive bricks was evaluated in terms of mean surface roughness and abrasive brick consumption occurred during polishing. SEM examinations revealed the evidences of the reasons that 25 wt% SiC powder embedded abrasive bricks has the best qualifications in terms of abrasion resistance and polishing performance.

REFERENCES

1. C. P. M. Tenorio, M. Dondi, G. Ercolani, G. Guarini, C. Melandri, M. Raimondo and E. R. Almendra, "The influence of microstructure on the performance of white porcelain stoneware", Ceramics International, Vol. 30, pp: 953–963, 2004.

2. E. Rambaldi, L. Esposito, A. Tucci and G. Timellini, "Recycling of polishing porcelain stoneware residues in ceramic tiles", Journal of the European Ceramic Society, Vol. 27, pp: 3509–3515, 2007.

3. I. M. Hutchings, K. Adachi, Y. Xu, E. Sanchez, M. J. Ibanez and M. F. Quereda, "Analysis and laboratory simulation of an industrial polishing process for porcelain ceramic tiles", Journal of the European Ceramic Society, Vol. 25, pp: 3151-3156, 2005.

4. J. Martin-Marquez, J. M. Rincon and M. Romero, "Effect of firing temperature on sintering of porcelain stoneware tiles", Ceramics International, Vol. 34, pp: 1867-1873, 2008.

5. M. Dondi, G. Ercolani, G. Guarini, C. Melandri, M. Raimondo, E. R. Almendra and P. M. Tenorio Cavalcante, "The role of surface microstructure on the resistance to stains of porcelain stoneware tiles", Journal of the European Ceramic Society, Vol. 25, pp: 357–365, 2005.

6. E. Sanchez, M. J. Ibanez, J. Garcıa-Ten, M.F. Quereda, I.M. Hutchings and Y. M. Xu, "Porcelain tile microstructure: Implications for polished tile properties", Journal of the European Ceramic Society, Vol. 26, pp: 2533–2540, 2006.

7. F. Andreola, L. Barbieri, E. Karamanova, I. Lancellotti and M. Pelino, "Recycling of CRT panel glass as fluxing agent in the porcelain stoneware tile production", Ceramics International, Vol. 34, pp: 1289–1295, 2008.

8. C. Leonelli, F. Bondioli, P. Veronesi, M. Romagnoli, T. Manfredini, G. C. Pellacani and V. Cannillo, “Enhancing the mechanical properites of porcelain stoneware tiles: a microstructural approach”, Journal of the European Ceramic Society, Vol. 21, pp: 785-793, 2001.

9. M. Romero, J. M. Marquez and J. M. Rincon, “Kinetic of mullite formation from a porcelain stoneware body for tiles production”, Journal of the European Ceramic Society, Vol. 26, pp: 1647–1652, 2006.

10. I. M. Hutchings, Y. Xua, E. Sanchez, M. J. Ibanez and M. F. Quereda, “Porcelain tile microstructure: implications for polishability”, Journal of the European Ceramic Society, Vol. 26, pp: 1035–1042, 2006.

11. L. Esposito, A. Tucci and D. Naldi, “The reliability of polished porcelain stoneware tiles”, Journal of the European Ceramic Society, Vol. 25, pp: 1487–1498, 2005.

12. E. Sanchez, J. Garcia-Ten, M. J Ibanez, M. J Orts and V. Cantavella, “Polishing porcelain tile (Part 1 wear mechanism)”, American Ceramic Society Bulletin, Vol. 81, pp: 50-54, 2002.

13. C. Y. Wang, X. Wei and H. Yuan, “Polishing of ceramic tiles”, Materials and Manufacturing Processes, Vol. 17, pp: 401-413, 2002.

14. Ö. Güzel and L. Gündüz, “Abrasives used in marble polishing cycles – an alternative matrix form analyses”, Türkiye III. Mermer Sempozyumu (Mersem 2001), pp: 249-263, 2001.

15. M. D. Casella, J. C. Lorentz, A. Traveria and J. M Tura, “Cracks in Sorel’s Cement polishing bricks as a result of magnesium oxychloride carbonatation”, Cement and Concrete Research, Vol. 26, pp: 1199-1202, 1996.

16. L. Zongjin and C. K. Chau, “Influence of molar ratios on properties of magnesium oxychloride cement”, Cement and Concrete Research, Vol. 37, pp: 866–870, 2007.

17. K. P. Maravelaki and G. Moraitou, “Sorel’s Cement mortars decay susceptibility and effect on pentelic marble”, Cement and Concrete Research, Vol. 29, pp: 1929–1935, 1999.

18. M. S. Özer, A. Göktaş, A. Öztürk and M. Timuçin, “Production and characterization of Sorel Cement based abrasive bricks for surface polishing of ceramic tiles”, SERES 2007 International Ceramic and Glaze Symposium, 2007.

19. M. S. Özer, A. Öztürk and M. Timuçin, “Formation and characterization of Sorel Cements”, International Symposium of Sustainability in Cement and Concrete, 2006.

20. Türk Standardları Enstitüsü, “TS 1769 Klinkerler- Sorel Çimentosu klinkeri (MgO)”, Ankara, 1994.

21. W. O. Robinson and W. H. Wingman, “Basic magnesium chlorides”, Journal of Physical Chemistry, Vol. 13, pp: 673-678, 1909.

22. C. R. Bury and E. R. H. Davies, “System magnesium oxide-magnesium chloride-water”, Journal of Chemical Society (London), pp: 2008-2015, 1932.

23. C. Harper, “Effect of calcination temperature on the properties of magnesium oxides for use in magnesium oxychloride cements”, Journal of Applied Chemistry, Vol. 17, pp: 5-10, 1967.

24. C. A. Sorrell and C. R. Armstrong, “Reactions and equilibria in magnesium oxychloride cements”, Journal of the American Ceramic Society, Vol. 59, pp: 51-54, 1976.

25. M. C. Ball, “Reactions of compounds occurring in Sorel’s Cement”, Cement and Concrete Research, Vol. 7, pp: 575-584, 1977.

26. L. Urwongse and C. A. Sorrell, “The system $MgO-MgCl_2-H_2O$ at 23 $^{\circ}C$”, Journal of the American Ceramic Society, Vol. 63, pp: 501-504, 1980.

27. C. Mazuranic, H. Bilinski and B. Matkovic, “Reaction products in the system $MgCl_2-NaOH-H_2O$”, Journal of the American Ceramic Society, Vol. 65, pp: 523-26, 1982.

28. H. Bilinski, B. Matkovic, C. Mazuranic and T. B. Zunic, “The formation of magnesium oxychloride phases in the systems $MgO-MgCl_2-H_2O$ and $NaOH-MgCl_2-H_2O$.” Journal of the American Ceramic Society, Vol. 67, pp: 266-269, 1984.

29. D. Dehua and Z. Chuanmei, “The formation mechanism of the hydrate phases in magnesium oxychloride cement”, Cement and Concrete Research, Vol. 29, pp: 1365–1371, 1999.

30. J. Yunsong, “A new type of light magnesium cement foamed material”, Materials Letters, Vol. 56, pp: 353– 356, 2002.

31. L. A. Skomorovskaya, T. S. Rudenko and E. A. Gabelkova: “Single firing of ceramic tiles for interior-wall facing”, An Imprint of Springer Verlag, New York LLC., Vol. 50, No. 7, pp: 304-305, 1993.

32. M. Llusar, C. Rodrigues, J. Labrincha, M. Flores and G. Monrós, “Reinforcement of single-firing ceramic glazes with the addition of polycrystalline tetragonal zirconia (3Y–TZP) or zircon”, Journal of European Ceramic Society, Vol. 22, pp: 639-652, 2002.

33. M. Llusar, G. Monrós, C. M. Rodrigues and J. A. Labrincha, "Study of zircon or zirconia crystals addition in ceramic glazes by impedance spectroscopy", Ceramic International, Vol. 31, pp: 181-188, 2005.

34. M. S. Gasser, G. H. A. Morad and H. F. Aly, "Batch kinetics and thermodynamics of chromium ions removal from waste solutions using synthetic adsorbents", Journal of Hazardous Materials, Vol. 142, pp: 118 –129, 2007.

35. D. Dehua, "The mechanism for soluble phosphates to improve the water resistance of magnesium oxychloride cement", Cement and Concrete Research, Vol. 33, pp: 1311 –1317, 2003.

36. P. Torres, H. R. Fernandes, S. Agathopoulos, D. U. Tulyaganov and J. M. F. Ferreira, "Incorporation of granite cutting sludge in industrial porcelain tile formulations", Journal of the European Ceramic Society, Vol. 24, pp: 3177–3185, 2004.

37. P. Torres, R. S. Manjate, S. Quaresma, H. R. Fernandes and J. M. F. Ferreira, "Development of ceramic floor tile compositions based on quartzite and granite sludges", Journal of the European Ceramic Society, Vol. 27, pp: 4649–4655, 2007.

38. E. Rambaldi, W. M. Carty, A. Tucci and L. Esposito, "Using waste glass as a partial flux substitution and pyroplastic deformation of a porcelain stoneware tile body", Ceramics International, Vol. 33, pp: 727–733, 2007.

39. D. Sarı and H. Yavuz, "Quantitative definition of marble gloss", Türkiye 3. Mermer Sempozyumu (Mersem 2001), pp: 265-275, 2001.

40. S. Dönmez and Y. D. Sarı, "3-Dimensional surface roughness measuring system", Teknoloji, Vol. 7, pp: 41-49, 2004.

41. W. Chang, “The effects of surface roughness and contaminants on the dynamic friction between porcelain tile and vulcanized rubber”, Safety Science, Vol. 40, pp: 577-591, 2002.

42. J. Li, G. Li and Y. Yu, “The influence of compound additive on magnesium oxychloride cement/urban refuse floor tile”, Construction and Building Materials, Vol. 22, pp: 521-525, 2008.

43. Greecian Magnesite Co., Products catologue (Coustic MgO).

44. Nedmag Industires Mining & Manufacturing B.V., Product data sheet ($MgCl_2$).

45. Akyol T.A.Ş. Products catologue (Zımpara kumu).

46. Eczacıbaşı Esan, Technical Data Sheet, No: TL.19.PS.70, 2005.

47. Türk Standardları Enstitüsü, “TS 1769 Klinkerler- Sorel Çimentosu Klinkeri (MgO)”, Ankara, 1994.

48. Türk Standardları Enstitüsü, “TS 699 - Tabii Yapı Taşları-Muayene ve Deney Metotları”, Ankara, 1987.

49. W. Fan, X. Song, S. Sun and X. Zhao, “Hydrothermal formation and characterization of magnesium hydroxide chloride hydrate nanowires”, Journal of Crystal Growth, Vol. 305, pp: 167–174, 2007.

50. L. J. Vandeperre, M. Liska and A. Al-Tabbaa, “Microstructures of reactive magnesia blends”, Cement and Concrete Composites, Vol. 30, pp: 706-714, 2008.

51. M. Masi, D. Colella, G. Radaelli and L. Bertolini, “Simulation of chloride penetration in cement-based materials”, Cement and Concrete Research, Vol. 27, pp: 1591-1601, 1997.

52. M. Lanzon and P. A. G. Ruiz, “Lightweight cement mortars: advantages and inconveniences of expanded perlite and its influence on fresh and hardened state and durability”, Construction and Building Materials, Vol. 22, pp: 1798-1806, 2008.

53. O. Bernard, F. J. Ulm and E. Lemarchand, “A multiscale micromechanics-hydration model for the early-age elastic properties of cement-based materials”, Cement and Concrete Research, Vol. 33, pp: 1293–1309, 2003.

54. G. Sant, C. F. Ferraris and J. Weiss, “Rheological properties of cement pastes: a discussion of structure formation and mechanical property development”, Cement and Concrete Research, Vol. 38, pp: 1286-1296, 2008.

55. X. Zhang and J. Han, “The effect of ultra-fine admixtures on the rheological property of cement paste”, Cement and Concrete Research, Vol. 30, pp: 827-830, 2000.

56. O. Özer and M. S. Kınkoğlu, “Türkiye'de üretilen magnezyaların Sorel Çimentosu parametrelerinin incelenmesi”, 4. Endüstriyel Hammaddeler Sempozyumu, 2001.

57. R. Gennaro, A. Langella, M. D. Amore, M. Dondi, A. Colella, P. Cappelletti and M. Gennaro, “Use of zeolite-rich rocks and waste materials for the production of structural lightweight concretes”, Applied Clay Science, Vol. 41, pp: 61-72, 2008.

58. S. Tsivilisa, J. Tsantilasa, G. Kakalia, E. Chaniotakisb and A. Sakellariou, “The permeability of Portland limestone cement concrete”, Cement and Concrete Research, Vol. 33, pp: 1465–1471, 2003.

59. S.P. Pandey, A. K. Singh, R. L. Sharma and A. K. Tiwari, “Studies on high-performance blended/multiblended cements and their durability characteristics”, Cement and Concrete Research, Vol. 33, pp: 1433–1436, 2003.

60. N. Bouzoubaa, M. H. Zhang and V. M. Malhotra, “Laboratory-produced high-volume fly ash blended cements compressive strength and resistance to the chloride-ion penetration of concrete”, Cement and Concrete Research, Vol. 30, pp: 1037-1046, 2000.

61. L. Basheer, P. A. M. Basheer and A. E. Long, “Influence of coarse aggregate on the permeation, durability and the microstructure characteristics of ordinary portland cement concrete”, Construction and Building Materials, Vol. 19, pp: 682–690, 2005.

62. J. W. Bullard and E. J. Garboczi, “A model investigation of the influence of particle shape on portland cement hydration”, Cement and Concrete Research, Vol. 36, pp: 1007-1015, 2006.

63. N. Bouzoubaa, M. H. Zhang and V. M. Malhotra, “Mechanical properties and durability of concrete made with high-volume fly ash blended cements using a coarse fly ash”, Cement and Concrete Research, Vol. 31, pp: 1393-1402, 2001.

64. J. M. Skibo, T. C. Butts and M. B. Schiffer, “Ceramic surface treatment and abrasion resistance: an experimental study”, Journal of Archaeological Science, Vol. 24, pp: 311-317, 1997.

65. C. Carde and R. Frarqois, “Modelling the loss of strength and porosity increase due to the leaching of cement pastes”, Cement and Concrete Composites, Vol. 21, pp: 181-188, 1999.

66. Z. Lafhaj, M. Goueygou, A. Djerbi and M. Kaczmarek, “Correlation between porosity, permeability and ultrasonic parameters of mortar with variable water/cement ratio and water content”, Cement and Concrete Research, Vol. 36, pp: 625-633, 2006.

67. C. Freidin, “Alkali-activated cement based on natural SiO_2-containing material Part I. strength, hydration, microstructure and durability”, Cement and Concrete Research, Vol. 33, pp: 1417-1422, 2003.